Experimental and Thermodynamic Constraints on the Sulphur Yield of Peralkaline and Metaluminous Silicic Flood Eruptions.

Bruno Scaillet, Ray Macdonald

▶ **To cite this version:**

Bruno Scaillet, Ray Macdonald. Experimental and Thermodynamic Constraints on the Sulphur Yield of Peralkaline and Metaluminous Silicic Flood Eruptions.. Journal of Petrology, 2006, 47, 7, pp.1413-1437. 10.1093/petrology/egl016 . hal-00022481

HAL Id: hal-00022481

https://hal-insu.archives-ouvertes.fr/hal-00022481

Submitted on 3 May 2006

HAL is a multi-disciplinary open access archive for the deposit and dissemination of scientific research documents, whether they are published or not. The documents may come from teaching and research institutions in France or abroad, or from public or private research centers.

L'archive ouverte pluridisciplinaire **HAL**, est destinée au dépôt et à la diffusion de documents scientifiques de niveau recherche, publiés ou non, émanant des établissements d'enseignement et de recherche français ou étrangers, des laboratoires publics ou privés.

Experimental and Thermodynamical Constraints on the Sulphur Yield of Peralkaline and Metaluminous Silicic Flood Eruptions

Bruno Scaillet[1] and Ray Macdonald[2]

[1*] Institut des Sciences de la Terre d'Orléans, UMR 6113 CNRS-UO, 1A rue de la Férollerie, 45071 Orléans, France

[2] Environment Centre, Lancaster University, Lancaster LA1 4YQ, UK

ABSTRACT

Many basaltic flood provinces are characterised by the existence of voluminous amounts of silicic magmas, yet the role of the silicic component in sulphur emissions associated with trap activity remains poorly known. We have performed experiments and theoretical calculations to address this issue. The melt sulphur content and fluid/melt partitioning at saturation with either sulphide or sulphate or both have been experimentally determined in three peralkaline rhyolites, which are a major component of some flood provinces. Experiments were done at 150 MPa, 800-900^{o}C, fO_2 in the range NNO-2 to NNO+3 and under water rich conditions. The sulphur content is strongly dependent on the peralkalinity of the melt, in addition to fO_2, and reaches 1000 ppm at NNO+1 in the most strongly peralkaline composition

at 800°C. At all values of fO_2, peralkaline melts can carry 5-20 times more sulphur than their metaluminous equivalents. Mildly peralkaline compositions show little variation in fluid/melt sulphur partitioning with changing fO_2 ($D_S \approx 270$). In the most peralkaline melt, D_S rises sharply at $fO_2 >$ NNO+1 to values of >500. The partition coefficient increases steadily for S_{bulk} between 1 and 6 wt% but remains about constant for S_{bulk} between 0.5 and 1 wt%. At bulk sulphur contents lower than 4 wt%, a temperature increase from 800 to 900°C decreases D_S by ~10%. *These results, along with (1) thermodynamic calculations on the behaviour of sulphur during the crystallisation of basalt and partial melting of the crust and (2) recent experimental constraints on sulphur solubility in metaluminous rhyolites, show that basalt fractionation can produce rhyolitic magmas having much more sulphur than rhyolites derived from crustal anatexis*. In particular, hot and dry metaluminous silicic magmas produced by melting of dehydrated lower crust are virtually devoid of sulphur. In contrast peralkaline rhyolites formed by crystal fractionation of alkali basalt can concentrate up to 90% of the original sulphur content of the parental magmas, especially when the basalt is CO_2-rich. On this basis, we estimate the amounts of sulphur potentially released to the atmosphere by the silicic component of flood eruptive sequences. The peralkaline Ethiopian and Deccan rhyolites

could have produced ~10^{17} and ~ 10^{18} g of S, respectively, which are comparable amounts to published estimates for the basaltic activity of each province. In contrast, despite similar erupted volumes, the metaluminous Paraná-Etendeka silicic eruptives could have injected only $4.6x10^{15}$ g of S in the atmosphere. Peralkaline flood sequences may thus have greater environmental effects than those of metaluminous affinity, in agreement with evidence available from mass extinctions and oceanic anoxic events.

INTRODUCTION

A detailed understanding of the solubility of sulphur in silicate melts is important for many geological processes (O'Neill & Mavrogenes, 2002): the origin of magmatic sulphide ores, the geochemical behaviour of the chalcophile trace elements, including the platinum group elements and the Re-Os isotopic system and their use as tracers of core-mantle and crust-mantle differentiation in the Earth and other planets or asteroids (e.g., Kracher & Wasson, 1982; Jana & Walker, 1997; Chabot, 2004). Sulphur solubility along with melt-vapor partitioning also determines sulphur degassing during volcanic activity and the potential effects on climate variability.

Most studies of sulphur solubility, cited in Carroll & Webster (1994), O'Neill & Mavrogenes (2002) and Jugo *et al*. (2005), have focussed on mafic and intermediate melt compositions. Our understanding of S behaviour in silicic magmas is more restricted and comes mainly from work on Fe-poor, metaluminous compositions (mol. $(CaO+Na_2O+K_2O) > Al_2O_3 > (Na_2O+K_2O)$), of the type commonly associated with volcanic arcs (Carroll & Rutherford, 1985; Luhr, 1990; Scaillet *et al*., 1998; Scaillet &

Evans, 1999; Keppler, 1999; Costa *et al*., 2004; Clemente *et al.,* 2004). Such compositions are not directly applicable to the magmatism of continental extensional zones, where the rhyolites tend to be alkali- and Fe-rich and either metaluminous or peralkaline (mol. $(Na_2O+K_2O) > Al_2O_3$) (Macdonald *et al*., 1992; King *et al*., 1997). The alkali/alumina balance of silicate melts is known to profoundly affect their geochemical and physical behaviour (Mysen, 1988). Most notable among those effects are the increase in Fe^{3+}/Fe^{2+} redox ratio (Gwin & Hess, 1989; Moore *et al*., 1995; Gaillard *et al*., 2001), water solubility (Dingwell *et al*., 1997), decrease of viscosity (Scarfe, 1977; Baker & Vaillancourt, 1995; Dingwell *et al*., 1998) and liquidus temperatures (Bailey & Schairer, 1966) as peralkalinity increases. These important differences imply that insight gained from the study of sulphur in metaluminous silicate melts is of little help in anticipating its behaviour in peralkaline rhyolites.

Whilst many flood basalt provinces seem to be dominated by basaltic lavas, several recent studies have emphasized that some have significant volumes of associated silicic rocks (Bellieni *et al*., 1986; Harris & Erlank, 1992; Peccerillo *et al*., 2003; Ewart *et al*., 1998, 2004; Ayalew *et al*., 2002; Bryan *et al*., 2002). The objective of the present study is to evaluate the sulphur yield potentially delivered to the atmosphere by silicic flood eruptions. Given that peralkaline rhyolites can largely dominate over metaluminous types in some silicic provinces (Ayalew *et al*., 2002), we currently lack the fundamental information on which to base any such evaluation. We have, therefore, performed melt solubility and fluid/melt partitioning experiments for sulphur in peralkaline rhyolites from the Kenya Rift Valley, which broadly typify the felsic end-member of bimodal associations in rift-related settings (Bellieni *et al*., 1986; Harris & Erlank, 1992; Peccerillo *et al*., 2003; Ewart *et al*., 1998, 2004; Ayalew *et al*., 2002; Bryan *et al*., 2002). We combine these data with thermodynamic and mass balance calculations to evaluate the sulphur contents of

potential sources of felsic magmas associated with flood basalts, considering two end-member cases for the origin of the silicic end-member: fractional crystallisation of flood basalt and partial melting of lower dehydrated crust. We show that the attainment of peralkaline conditions dramatically increases the sulphur-carrying capacity of rhyolite magmas. We then estimate the sulphur yields of some silicic flood sequences. The results appear to be significant for the current debate on the volcanic origin of some of the main mass extinctions (e.g. Wignall, 2001; Morgan *et al*., 2004).

EXPERIMENTAL AND ANALYTICAL TECHNIQUES

We have performed sulphur solubility and fluid/melt partitioning experiments on three well-characterised, peralkaline rhyolitic obsidians from the Naivasha area of the Kenya Rift Valley (Table 1).

Table 1. ***Experimental conditions, masses of silicate and volatiles, run products and phase proportions***

charge	P tot bar	fH_2 bar	fH_2O bar	T °C	ΔNNO	duration hr	S bulk wt%	silicate+S mg	H_2O mg	sulphur mg	fl wt%	Po wt%
ND bulk												
ND-1	**1520**	**40.0**	**1166**	**803**	**-1.61**	**165**	**1.01**	**20.20**	**1.90**	**0.20**	**3.89**	**1.65**
ND-2	**1500**	**7.7**	**1180**	**803**	**-0.17**	**172**	**1.01**	**19.60**	**2.00**	**0.20**	**4.59**	**1.65**
ND-4	**1520**	**2.5**	**1170**	**804**	**0.82**	**309**	**1.01**	**20.00**	**2.10**	**0.20**	**4.90**	**1.47**
ND-5	**1520**	**1.3**	**1177**	**803**	**1.37**	**193**	**1.01**	**20.30**	**2.00**	**0.20**	**4.17**	**1.45**
ND-6	**1520**	**0.5**	**1120**	**806**	**2.25**	**192**	**1.01**	**20.30**	**2.00**	**0.20**	**4.63**	**-**
ND-3	**1500**	**0.2**	**1123**	**808**	**2.96**	**188**	**1.01**	**30.00**	**3.00**	**0.30**	**4.73**	**-**
ND-9	**1561**	**50.0**	**1295**	**900**	**-1.63**	**96**	**1.01**	**20.10**	**2.00**	**0.20**	**4.94**	**1.38**
SMN-bulk												
SMN-1	**1520**	**40.0**	**1182**	**803**	**-1.60**	**165**	**1.19**	**19.80**	**2.10**	**0.24**	**4.92**	**2.16**
SMN-2	**1500**	**7.7**	**1149**	**803**	**-0.19**	**172**	**1.19**	**20.20**	**2.00**	**0.24**	**4.39**	**1.93**
SMN-4	**1520**	**2.5**	**1150**	**804**	**0.80**	**309**	**1.19**	**20.70**	**2.00**	**0.25**	**4.23**	**1.76**
SMN-5	**1520**	**1.3**	**1120**	**803**	**1.33**	**193**	**1.19**	**19.20**	**2.20**	**0.23**	**6.24**	**-**
SMN-6	**1520**	**0.5**	**1098**	**806**	**2.24**	**192**	**1.19**	**20.40**	**2.10**	**0.24**	**5.24**	**-**
SMN-3	**1500**	**0.2**	**1098**	**808**	**2.94**	**188**	**1.19**	**20.20**	**2.10**	**0.24**	**5.32**	**-**

SMN-9	**1561**	**50.0**	**1299**	**900**	**-1.63**	**96**	**1.19**	**20.00**	**2.00**	**0.24**	**4.60**	**1.65**
EBU bulk												
EBU-1	**1520**	**40.0**	**1205**	**803**	**-1.58**	**165**	**1.08**	**21.00**	**2.00**	**0.23**	**3.78**	**2.31**
EBU-2	**1500**	**7.7**	**1181**	**803**	**-0.17**	**172**	**1.08**	**20.20**	**2.00**	**0.22**	**4.18**	**2.06**

Table 1. Continued

charge	**P tot bar**	***f*H_2 bar**	***f*H_2O bar**	**T °C**	**ΔNNO**	**duration hr**	**S bulk wt%**	**silicate+S mg**	**H_2O mg**	**sulphur mg**	**fl wt%**	**Po wt%**
EBU-4	**1520**	**2.5**	**1159**	**804**	**0.81**	**309**	**1.08**	**20.60**	**2.00**	**0.22**	**4.23**	**1.45**
EBU-5	**1520**	**1.3**	**1104**	**803**	**1.32**	**193**	**1.08**	**20.80**	**2.10**	**0.22**	**4.99**	**-**
EBU-6	**1520**	**0.5**	**1074**	**806**	**2.22**	**192**	**1.08**	**21.10**	**1.90**	**0.22**	**4.02**	**-**
EBU-3	**1500**	**0.2**	**1093**	**808**	**2.94**	**188**	**1.08**	**20.40**	**2.00**	**0.22**	**4.74**	**-**
EBU-7-0.5	**1500**	**6.1**	**1195**	**801**	**0.04**	**214**	**0.50**	**20.40**	**2.10**	**0.10**	**4.45**	**0.82**
EBU-7-2	**1500**	**6.1**	**1133**	**801**	**0.00**	**214**	**2.01**	**20.70**	**2.00**	**0.42**	**4.25**	**3.66**
EBU-7-4	**1500**	**6.1**	**1003**	**801**	**-0.11**	**214**	**3.85**	**20.10**	**1.90**	**0.77**	**4.94**	**6.01**
EBU-7-6	**1500**	**6.1**	**890**	**801**	**-0.21**	**214**	**6.14**	**20.00**	**2.10**	**1.23**	**7.43**	**7.40**
EBU-8-2	**1510**	**44.0**	**1161**	**805**	**-1.70**	**183**	**2.01**	**20.70**	**2.10**	**0.42**	**4.58**	**4.08**
EBU-8-4	**1510**	**44.0**	**1047**	**805**	**-1.79**	**183**	**3.85**	**21.30**	**2.10**	**0.82**	**5.12**	**6.51**
EBU-8-6	**1510**	**44.0**	**825**	**805**	**-1.99**	**183**	**6.14**	**21.50**	**2.00**	**1.32**	**6.41**	**7.31**

EBU-9-0.5	**1561**	**55.0**	**1353**	**900**	**-1.60**	**96**	**0.50**	**21.00**	**2.00**	**0.11**	**3.78**	**1.00**
EBU-9-1	**1561**	**50.0**	**1328**	**900**	**-1.61**	**96**	**1.08**	**20.00**	**2.00**	**0.22**	**4.35**	**2.07**
EBU-9-2	**1561**	**50.0**	**1253**	**900**	**-1.66**	**96**	**2.01**	**22.60**	**2.10**	**0.45**	**4.07**	**3.52**
EBU-9-4	**1561**	**50.0**	**1119**	**900**	**-1.76**	**96**	**3.85**	**20.90**	**2.00**	**0.80**	**5.22**	**5.71**
EBU-9-6	**1561**	**50.0**	**934**	**900**	**-1.92**	**96**	**6.14**	**20.40**	**2.00**	**1.25**	**7.22**	**6.56**

S bulk is the wt% content of sulphur of the silicate powder. The mass of sulphur in the charge is given in the column labelled sulphur.
The wt% of pyrrhotite (Po), anhydrite (Anhy) and oxide (Ox) are calculated on the basis of condensed phases only (i.e. hydrous glass + minerals).
fl is the weigth % of fluid at P and T.

Two (ND, SMN) are mildly peralkaline comendites ($(Na_2O+K_2O)/Al_2O_3$ = 1.05 and 1.31, respectively) from the Greater Olkaria Volcanic Complex and were previously used in phase equilibrium studies (Scaillet & Macdonald, 2001; 2003). The third, EBU, is a pantelleritic obsidian from a welded fall deposit of the Eburru Volcanic Complex, immediately north of Olkaria. It is more strongly peralkaline than the comendites (NK/A = 1.88) and represents a composition that could have been generated by ~50% crystallization of Olkaria-type comendites similar to SMN (Scaillet & Macdonald, 2003). These starting melt compositions (Table 1) encompass the entire peralkalinity range displayed by rhyolites associated with flood basalts (Trua *et al*., 1999; Ayalew *et al*., 2002; Peccerillo *et al*., 2003). We restricted our investigations to low pressure conditions (~150 MPa), thought to be relevant to the production of alkali rhyolites (Mahood, 1984; Scaillet & Macdonald, 2001) and we focussed on the role of oxygen fugacity (fO_2), which exerts a strong control on sulphur behaviour in silicic magmas (e.g., Carroll & Webster, 1994 ; Scaillet *et al*., 1998; Keppler, 1999).

The experimental procedures are similar to those used in previous studies performed at the ISTO experimental petrology laboratory, such as that by Scaillet *et al*. (1998) and Clemente *et al*. (2004). For each composition, batches of starting glass+sulphur powders with fixed sulphur contents were prepared by weighing 200 mg of glass powder with appropriate amounts of elemental sulphur (1 to 12 mg added sulphur). The resulting mixture was thoroughly mixed in an agate mortar for several minutes. Most experiments used ND, SMN and EBU batches with bulk sulphur contents of *c.* 1 wt% (1.01, 1.19 and 1.08 wt%, respectively see Table 1). However, two series with EBU composition were performed with additional bulk sulphur contents of 0.5, 2.01, 3.85 and 6.14 wt% S, so as to explore the effect of sulphur fugacity at fixed P and T and fH_2. We used Au capsules, which were loaded with the glass+sulphur powder (*c.* 20-30 mg, Table 1) plus weighed amounts of distilled water *(c*. 10 wt%, Table 1), and welded shut with a graphite arc welder. Weighing before and after welding, as well as after run completion, was used as a monitor for any volatile loss having occurred at P and T. For all charges used in this study, capsule weighs remained constant to within 0.2 mg. We used either cold seal pressure vessels (CSPV) fitted with an H_2 membrane

(runs at 800°C) or an internally heated pressure vessel (IHPV) with a drop quench setting (900°C). Errors in quoted temperatures and pressures are ±8°C, and 2 MPa, respectively. The fO_2 was varied using various Ar-H_2 mixtures as the pressurizing gas. The H_2 fugacity was either read with an H_2-membrane (800°C) or known from previous experiments that used the same Ar-H_2 ratio and which were run with an H_2 membrane (900°C). Errors on H_2 fugacities are ±0.01 MPa (800°C), or ±0.5 MPa (900°C), the latter determined by repeat experiments performed with the IHPV while fitted with a H_2 membrane. The fO_2 of each charge was computed using the dissociation reaction of water (Robie *et al*., 1979), the fH_2 and the water fugacity (fH_2O). The fH_2O of each charge (Table 1) was computed assuming ideal behaviour in the fluid (i.e., $aH_2O=XH_2O_{fl}$, XH_2O_{fl} being the mole fraction of H_2O in the fluid and aH_2O the activity of water defined as the ratio $fH_2O/fH_2O°$, $fH_2O°$ being the fugacity of pure water at P and T as given by Burnham *et al*. (1969)) and using the calculated fluid composition as determined from mass balance constraints. The fluid composition was calculated knowing the amounts of dissolved water and sulphur, the amount of sulphur locked into solid phases (sulphide and sulphate) and the bulk content of water and sulphur loaded to the capsules. The water content of quenched melts (glasses) was determined using the by-difference method employing appropriate sets of hydrous glass standards of known H_2O contents (Scaillet & Macdonald, 2001). For charges with *c*. 1 wt% bulk sulphur, the calculated XH_2O_{fl} of the equilibrium fluid (Table 2) is close to, or higher than, 0.9, with the result that the calculated fO_2 is only marginally lower than that corresponding to pure H_2O (difference less than 0.05 log unit). For those charges we estimate that the uncertainty on fO_2 is < 0.1 log units. In contrast, charges having bulk sulphur contents in excess of 1 wt% have calculated fluid compositions that are significantly poorer in H_2O, with XH_2O_{fl} going down to 0.68 (Table 2).

Table 2. **Compositions of glasses, coexisting fluid, and calculated fluid/melt sulphur partition coefficients**

charge	SiO_2	Al_2O_3	FeO	MgO	CaO	Na_2O	K_2O	F	Cl	NK/A	n	S_{melt}	S_{fluid}	X_{H2Ofl}	S_{fl}/S_{melt}
	wt%	wt%	wt%	wt%	wt%	wt%	wt%	wt%	wt%			ppm	wt%		
ND bulk	**75.20**	**12.11**	**1.81**	**0.07**	**0.44**	**4.59**	**4.73**	**0.37**	**0.22**	**1.05**					
ND-1	**77.25**	**12.08**	**0.39**	**0.05**	**0.37**	**4.54**	**5.00**	**0.13**	**0.13**	**1.07**	**7**	**268**	***8.2***	***0.95***	***307***
	0.18	***0.12***	***0.08***	***0.03***	***0.05***	***0.01***	***0.08***	***0.14***	***0.03***			***31***			
ND-2	**77.18**	**12.17**	**0.39**	**0.05**	**0.35**	**4.55**	**4.98**	**0.13**	**0.13**	**1.06**	**7**	**265**	***6.9***	***0.96***	***261***
	0.22	***0.13***	***0.19***	***0.03***	***0.05***	***0.01***	***0.12***	***0.10***	***0.04***			***34***			
ND-4	**77.25**	**12.19**	**0.54**	**0.04**	**0.30**	**4.54**	**4.76**	**0.18**	**0.15**	**1.03**	**12**	**266**	***7.7***	***0.96***	***290***
	0.21	***0.15***	***0.17***	***0.03***	***0.06***	***0.01***	***0.12***	***0.09***	***0.04***			***36***			
ND-5	**77.43**	**12.20**	**0.56**	**0.05**	**0.09**	**4.53**	**4.72**	**0.22**	**0.08**	**1.03**	**10**	**329**	***4.8***	***0.97***	***147***
	0.08	***0.16***	***0.12***	***0.02***	***0.03***	***0.00***	***0.08***	***0.10***	***0.04***			***42***			
ND-6	**77.43**	**12.16**	**0.87**	**0.03**	**0.03**	**4.51**	**4.55**	**0.16**	**0.11**	**1.02**	**10**	**462**	***14.4***	***0.91***	***310***
	0.27	***0.13***	***0.14***	***0.02***	***0.03***	***0.01***	***0.23***	***0.13***	***0.06***			***27***			
ND-3	**77.33**	**12.19**	**0.78**	**0.02**	**0.01**	**4.53**	**4.67**	**0.25**	**0.05**	**1.03**	**6**	**633**	***13.4***	***0.92***	***212***
	0.25	***0.09***	***0.13***	***0.02***	***0.02***	***0.01***	***0.16***	***0.16***	***0.03***			***38***			
ND-9	**76.97**	**11.98**	**0.63**	**0.04**	**0.37**	**4.55**	**4.82**	**0.27**	**0.12**	**1.06**	**7**	**303**	***8.9***	***0.95***	***294***
	0.23	***0.13***	***0.10***	***0.03***	***0.06***	***0.01***	***0.12***	***0.05***	***0.05***			***15***			
SMN-bulk	**74.17**	**10.89**	**3.98**	**0.00**	**0.29**	**5.81**	**4.34**	**1.00**	**0.50**	**1.31**					
SMN-1	**75.60**	**10.67**	**2.11**	**0.02**	**0.06**	**5.71**	**4.45**	**1.07**	**0.26**	**1.33**	**7**	**242**	***6.1***	***0.97***	***254***
	0.24	***0.12***	***0.23***	***0.02***	***0.05***	***0.01***	***0.16***	***0.14***	***0.08***			***39***			
SMN-2	**75.14**	**10.66**	**2.32**	**0.01**	**0.06**	**5.72**	**4.42**	**1.17**	**0.37**	**1.33**	**8**	**315**	***8.7***	***0.95***	***277***
	0.36	***0.12***	***0.28***	***0.01***	***0.04***	***0.01***	***0.20***	***0.20***	***0.12***			***24***			
SMN-4	**75.23**	**10.75**	**2.46**	**0.01**	**0.03**	**5.70**	**4.33**	**1.20**	**0.22**	**1.31**	**16**	**351**	***10.3***	***0.94***	***293***
	0.22	***0.10***	***0.11***	***0.01***	***0.03***	***0.01***	***0.12***	***0.15***	***0.06***			***67***			
SMN-5	**75.43**	**10.53**	**2.67**	**0.02**	**0.03**	**5.67**	**4.20**	**1.09**	**0.21**	**1.32**	**10**	**452**	***14.4***	***0.91***	***318***
	0.26	***0.15***	***0.25***	***0.01***	***0.02***	***0.01***	***0.16***	***0.07***	***0.06***			***46***			
SMN-6	**76.51**	**10.73**	**1.58**	**0.00**	**0.01**	**5.65**	**4.24**	**1.08**	**0.08**	**1.29**	**10**	**487**	***17.1***	***0.90***	***350***
	0.22	***0.15***	***0.14***	***0.01***	***0.02***	***0.01***	***0.11***	***0.10***	***0.02***			***37***			

charge	SiO_2	Al_2O_3	FeO	MgO	CaO	Na_2O	K_2O	F	Cl	NK/A	n	S_{melt}	S_{fluid}	X_{H2Ofl}	S_{fl}/S_{melt}
SMN-3	**76.53**	**10.86**	**1.49**	**0.01**	**0.00**	**5.67**	**4.16**	**0.89**	**0.15**	**1.27**	**6**	**550**	***16.7***	***0.90***	***303***
	0.25	***0.10***	***0.14***	***0.01***	***0.01***	***0.01***	***0.12***	***0.22***	***0.06***			***24***			

SMN-9	**75.22**	**10.49**	**2.35**	**0.02**	**0.06**	**5.74**	**4.41**	**1.05**	**0.41**	**1.36**	**8**	**548**	**11.0**	**0.94**	**201**
	0.24	***0.16***	***0.21***	***0.02***	***0.02***	***0.01***	***0.15***	***0.16***	***0.05***			***46***			
EBU bulk	**70.86**	**8.48**	**7.17**	**0.52**	**0.30**	**6.68**	**4.50**	**0.78**	**0.43**	**1.87**					
EBU-1	**74.09**	**8.30**	**5.19**	**0.01**	**0.23**	**6.52**	**4.41**	**0.79**	**0.35**	**1.87**	**6**	**738**	**2.8**	**0.98**	**38**
	0.23	***0.10***	***0.28***	***0.01***	***0.05***	***0.01***	***0.11***	***0.19***	***0.07***			***65***			
EBU-2	**73.37**	**8.38**	**5.40**	**0.01**	**0.28**	**6.54**	**4.41**	**0.96**	**0.36**	**1.85**	**7**	**897**	**4.3**	**0.98**	**48**
	0.32	***0.06***	***0.25***	***0.02***	***0.04***	***0.03***	***0.08***	***0.11***	***0.08***			***37***			
EBU-4	**73.75**	**8.29**	**5.93**	**0.01**	**0.14**	**6.50**	**4.19**	**0.82**	**0.23**	**1.84**	**11**	**928**	**9.3**	**0.95**	**100**
	0.34	***0.07***	***0.25***	***0.01***	***0.04***	***0.01***	***0.13***	***0.09***	***0.04***			***67***			
EBU-5	**75.37**	**8.45**	**4.68**	**0.02**	**0.05**	**6.47**	**4.03**	**0.70**	**0.16**	**1.77**	**10**	**549**	**16.3**	**0.90**	**297**
	0.22	***0.06***	***0.13***	***0.02***	***0.02***	***0.01***	***0.11***	***0.14***	***0.01***			***25***			
EBU-6	**75.65**	**8.46**	**4.43**	**0.02**	**0.02**	**6.46**	**4.05**	**0.66**	**0.12**	**1.78**	**11**	**368**	**19.9**	**0.88**	**542**
	0.22	***0.21***	***0.22***	***0.02***	***0.02***	***0.01***	***0.09***	***0.12***	***0.02***			***23***			
EBU-3	**75.60**	**8.50**	**4.51**	**0.01**	**0.04**	**6.47**	**3.95**	**0.78**	**0.11**	**1.76**	**5**	**434**	**17.3**	**0.90**	**399**
	0.39	***0.09***	***0.28***	***0.01***	***0.04***	***0.01***	***0.13***	***0.18***	***0.05***			***17***			
EBU-7-0.5	**72.92**	**8.13**	**6.47**	**0.01**	**0.26**	**6.52**	**4.31**	**0.87**	**0.33**	**1.89**	**11**	**744**	**2.2**	**0.99**	**30**
	0.39	***0.08***	***0.26***	***0.02***	***0.05***	***0.02***	***0.15***	***0.17***	***0.04***			***72***			
EBU-7-2	**75.01**	**8.43**	**4.03**	**0.03**	**0.21**	**6.53**	**4.32**	**0.89**	**0.31**	**1.83**	**13**	**1013**	**10.8**	**0.94**	**107**
	0.20	***0.12***	***0.14***	***0.01***	***0.02***	***0.01***	***0.21***	***0.19***	***0.09***			***149***			
EBU-7-4	**77.29**	**8.59**	**2.00**	**0.02**	**0.11**	**6.50**	**4.44**	**0.66**	**0.15**	**1.81**	**10**	**845**	**26.9**	**0.83**	**319**
	0.30	***0.16***	***0.16***	***0.02***	***0.03***	***0.01***	***0.13***	***0.18***	***0.03***			***61***			
EBU-7-6	**78.70**	**8.77**	**0.79**	**0.01**	**0.08**	**6.48**	**4.39**	**0.46**	**0.08**	**1.76**	**10**	**880**	**39.1**	**0.74**	**445**
	0.23	***0.09***	***0.11***	***0.02***	***0.02***	***0.02***	***0.09***	***0.13***	***0.01***			***94***			

charge	**SiO_2**	**Al_2O_3**	**FeO**	**MgO**	**CaO**	**Na_2O**	**K_2O**	**F**	**Cl**	**NK/A**	**n**	**S_{melt}**	**S_{fluid}**	**X_{H2Ofl}**	**S_{fl}/S_{melt}**
	wt%	**wt%**	**wt%**	**wt%**	**wt%**	**wt%**	**wt%**	**wt%**	**wt%**			**ppm**	**wt%**		
EBU-8-2	**74.92**	**8.49**	**3.66**	**0.02**	**0.28**	**6.57**	**4.48**	**1.04**	**0.42**	**1.84**	**10**	**445**	**7.9**	**0.95**	**177**
	0.19	***0.10***	***0.15***	***0.02***	***0.04***	***0.01***	***0.12***	***0.11***	***0.07***			***56***			
EBU-8-4	**76.83**	**8.69**	**1.57**	**0.01**	**0.26**	**6.58**	**4.53**	**0.90**	**0.35**	**1.81**	**12**	**891**	**22.4**	**0.86**	**252**
	0.48	***0.11***	***0.18***	***0.01***	***0.07***	***0.03***	***0.11***	***0.23***	***0.10***			***148***			
EBU-8-6	**77.49**	**8.67**	**0.87**	**0.01**	**0.28**	**6.62**	**4.54**	**0.84**	**0.33**	**1.82**	**13**	**1222**	**45.7**	**0.68**	**374**
	0.36	***0.18***	***0.06***	***0.02***	***0.07***	***0.01***	***0.13***	***0.15***	***0.04***			***180***			
EBU-9-0.5	**72.66**	**8.06**	**6.32**	**0.02**	**0.23**	**6.55**	**4.30**	**0.82**	**0.41**	**1.92**	**8**	**969**	**2.8**	**0.98**	**29**
	0.28	***0.07***	***0.14***	***0.03***	***0.03***	***0.00***	***0.15***	***0.10***	***0.03***			***52***			
EBU-9-1	**73.34**	**8.10**	**5.39**	**0.01**	**0.26**	**6.57**	**4.37**	**0.84**	**0.44**	**1.92**	**8**	**1032**	**5.9**	**0.97**	**58**

	0.11	*0.13*	*0.18*	*0.01*	*0.04*	*0.02*	*0.12*	*0.04*	*0.04*			*25*			
EBU-9-2	**74.44**	**8.23**	**4.15**	**0.01**	**0.27**	**6.58**	**4.38**	**0.77**	**0.42**	**1.89**	**8**	**1193**	**14.8**	**0.91**	**124**
	0.35	*0.07*	*0.19*	*0.02*	*0.07*	*0.01*	*0.11*	*0.07*	*0.07*			*43*			
EBU-9-4	**76.00**	**8.45**	**2.25**	**0.02**	**0.25**	**6.62**	**4.59**	**0.71**	**0.36**	**1.88**	**9**	**1591**	**28.9**	**0.81**	**182**
	0.24	*0.05*	*0.17*	*0.02*	*0.06*	*0.02*	*0.15*	*0.06*	*0.06*			*73*			
EBU-9-6	**76.39**	**8.49**	**1.52**	**0.02**	**0.26**	**6.63**	**4.54**	**0.74**	**0.37**	**1.87**	**8**	**2254**	**45.8**	**0.68**	**203**
	0.31	*0.03*	*0.27*	*0.03*	*0.03*	*0.00*	*0.20*	*0.13*	*0.04*			*47*			

Glass compositions have been normalised to 100% anhydrous. Melt water contents determined with the by-difference method range from 5 to 6 wt%. The 1 standard deviation of each oxide or element analysed is given in italics below the concentration. Reported glass compositions are average of 6-10 electron microprobe analyses
The XH_2O_{fl} represents the mole fraction of H_2O of the coexisting fluid phase that is made of H_2O and H_2S (low fO_2) or SO_2 (high fO_2), and which is determined by mass balance.
The S_{melt} and S_{fluid} are the sulphur content of melt and fluid, respectively.
n is the number of electron microprobe analyses of sulphur.
NK/A is the $(Na_2O+K_2O)/Al_2O_3$ ratio (moles).

As a result, the value of fO_2 for the sulphur-rich charges is lower than that corresponding to the pure H_2O case. However, for a fixed set of P-T-fH_2 conditions (i.e. series EBU-9 in Table 1), the difference in calculated fO_2 between the sulphur-poor and sulphur-rich charges does not exceed 0.3 log unit (Table 1). *The main source of uncertainty in S-rich charges comes from the estimate of the amount of H_2O dissolved in the melt. An error of 1 wt% absolute (i.e. 4.5 wt% instead of 5.5 wt%) produces a change in calculated XH_2O_{fl} of about ± 0.07, which in turn induces a change in the calculated log fO_2 of about ± 0.07 unit. Overall, for the sulphur-rich charges we estimate that the fO_2 is known to within 0.3 log unit.*

Because we use elemental sulphur as a source of sulphur, and not either sulphide or anhydrite (e.g. Luhr, 1990), the initial redox state of the charges is grossly out of equilibrium since the sulphur in the fluid must be complexed either with O_2 to form SO_2 or with H_2 to produce H_2S, which are the two dominant fluid species in the fluid at P and T, depending on fO_2 (see Clemente et al., 2004). As long as H_2 from the vessel does not diffuse across the capsule walls (i.e. below 600°C), the redox state of the charges will be internally controlled to some value which will depend on factors such as the ratio of H_2O to S loaded, the amount of atmospheric O_2 present in the capsule and the rates of H_2O and S dissolution into glass/melt. At 800°C, however, the kinetics of H_2 diffusion even within Au is so fast that osmotic equilibrium in H_2 is attained within a few tens of seconds across capsule walls (Scaillet et al., 1992), and maintained at a fixed value owing to the large H_2-buffering capacity of the vessel volume (Schmidt et al., 1995). Both the CSPV and IHPV attain the target temperature in about 20 min, so that the period elapsed at low temperature conditions, during which transient redox state may occur, is short relative to the total run duration (minimum of 96 hrs, Table 1). Redox equilibrium will be reached as soon as the dissolution process of volatiles into melt is achieved. Using appropriate diffusivities for H_2O and S (taken at 800°C as 10^{-7} cm^2/s and 10^{-9} cm^2/s, respectively (Watson, 1994)), it can be calculated that volatile dissolution occurs in a matter of minutes (H_2O) to few hours (S) owing to the finely powdered and well mixed nature of our starting material, which minimises the diffusion length scale of volatiles to a few tens of microns. None of the

charges produced in this study displayed textural evidence of redox disequilibrium such as sulphide rimmed by sulphate or vice versa, suggesting that either the charge has no time to record redox states radically different from that imposed at run conditions, or any evidence of such variations in fO_2 during the heating-up period has been erased upon run completion.

Run products were characterised first by optical inspection with a metallographic microscope and then by electron microprobe analysis (EMPA). Observation under reflected light prior to carbon-coating allowed the oxide to be distinguished easily from sulphide owing to their contrasted colours (grey for oxide *vs*. yellowish for sulphide) as well as shape (rectangular to equant shape for oxide *vs* pentagonal to rounded shape for smaller individual sulphide grain). Investigation under transmitted light and crossed polars enabled straightforward identification of anhydrite in oxidized charges due to its high birefringence. In anhydrite-bearing charges, anhydrite was fully enclosed by glass, suggesting that it grew from melt and is not the result of back reaction of fluid upon cooling, in which cases it should have partially filled open cavities representing former gas bubbles. In all cases, optical identification of minerals was confirmed by subsequent EMPA, although owing to their generally small size, most analyses of minerals were contaminated by glass. We used the following conditions to determine the composition of glasses. For major elements, the conditions were: accelerating voltage 15 kV, sample current 6 nA, counting time 10 s on peak for all elements, and a beam defocused to 5 □m. Na and K were analysed first and a ZAF correction procedure applied. Correction factors for Na loss were based on analyses of synthetic peralkaline rhyolitic compositions and a set of metaluminous rhyolitic and dacitic glasses, all of known water content as determined by Karl Fischer titration. Between 6 and 10 analyses were performed for each glass. The water content of quenched glasses varied between 5 and 6 wt%, except for the two charges with *c.* 6 wt% sulphur which displayed slightly lower values (between 4 and 5 wt%). Owing to the large uncertainties of the by-difference technique in determining the H_2O content of quenched glasses (e.g. Devine *et al*., 1995), in this work we use a fixed melt water content of 5.5 wt% for all charges. The concentration of total sulphur in glasses was determined by EMPA using 3 synthetic hydrous dacitic glasses containing 750, 1400, and 1900

ppm sulphur (determined by wet chemistry) as standards (Clemente *et al*., 2004). The EMPA was run with the following conditions: accelerating voltage 15 kV, sample current 50 nA, beam diameter 10 μm with a counting time of 60 s. The background was determined by analysing a dry rhyolitic glass without sulphur, using the above analytical procedure. The detection limit under these analytical conditions is about 80 ppm. The sulphur data given in Table 2 are averages of 5-16 analyses.

Apart from oxide and sulphur-bearing phases, no other mineral was detected. Two S-bearing phases crystallised: pyrrhotite at NNO <1 and anhydrite at NNO >1. At high fO_2, an oxide co-precipitated with anhydrite. Knowing the amount of sulphur-bearing phases crystallised, and the amount of sulphur dissolved in the melt, the sulphur content of the coexisting fluid is calculated by difference with the known bulk sulphur content, using stoichiometric FeS and $CaSO_4$ as sulphide or sulphate minerals (e.g., Scaillet *et al*., 1998). Since, depending on fO_2, sulphide or sulphate+oxides were the sole phases crystallising (Table 1), the maximum proportions of sulphur-bearing minerals can be determined by the changes in either FeO_{tot} (fO_2 < NNO) or CaO (fO_2 > NNO+1) of the quenched glass. This obviously assumes that neither iron or calcium is transported into the fluid (or lost to the capsule in the case of iron but, under our experimental conditions, sulphur was never detected in Au capsules). If any of these two elements is partitioned into the fluid, the amounts of sulphide or sulphate calculated from variations in FeO and CaO abundances in glass will be overestimated, with the consequence that there will be too much sulphur locked in solid phases. As a result, the calculated partition coefficient will be lower than its real value. Conversely, as stated above, we assume that pyrrhotite is end-member FeS. Pyrrhotite departure from FeS stoichiometry can be up to Fe_5S_6. An Fe_5S_6 stoichiometry would decrease our calculated partition coefficients, since it maximises the amount of sulphur tied up with iron in pyrrhotite and this sulphur is therefore no longer available to the fluid. For charges saturated in anhydrite, a problem also arises from the low bulk CaO content of the starting rocks. Generally those charges have melts with CaO contents close to the detection limit. The fact that this extreme depletion in CaO goes along with a decrease in melt Cl content relative to the starting value (see Table 2), suggests that not all the Ca complexes with sulphur to form anhydrite but that some goes into the fluid,

possibly as $CaCl_2$ species. The concentration of CaO in charges run at low fO_2 remains close to the starting value, although some depletion does occur, possibly also as a result of Ca complexing with Cl. We recognise that partition coefficients of sulphur between fluid and melt determined in this way (by default) can be affected by a number of errors, as illustrated below. However, there is unfortunately no straightforward way of assessing this parameter in hydrothermal experiments. In particular, measuring the H-O-S fluid compositions upon quench is unlikely to retrieve the correct numbers since back reactions within fluid can alter both its speciation and composition (L. Baker, personal communication).

As an example consider charge ND1 whose partition coefficient, Ds, calculated using the above assumptions, is 307 (Table 1). This charge consisted of 20.2 mg of silicate powder with 1.01 wt% S (0.2 mg), and 1.9 mg of H_2O. The bulk FeO is 1.81 wt% (0.37 mg) and after the run the hydrous glass (5.5 wt% or 1.11 mg H_2O) has 0.39 wt% FeO_{tot} (0.08 mg). The difference in FeO content in glass before and after the run (0.2867 mg) implies that 0.00399 milimole of Fe is sequestered in pyrrhotite (0.2867/71.85). Assuming stoichiometric pyrrhotite this implies in turn that 0.128 mg (32x0.004) of sulphur is locked up in pyrrhotite. Knowing that the glass has 268 ppm dissolved sulphur, corresponding to 0.0054 mg sulphur, this leaves 0.07 mg sulphur for the fluid (or 0.074 mg H_2S). The amount of water in the fluid is 0.79 mg (1.9-1.11), which implies that the mole fraction of H_2O in the fluid, XH_2O, is 0.95, and that the amount of fluid at P and T is 0.864 mg (0.79+0.074) which corresponds to 3.9 wt% fluid in the system (0.864/(20.2+1.9)), the fluid having 8.2 wt% sulphur. *The amount of pyrrhotite is 1.65 wt%, calculated on the basis of condensed phases only (hydrous glass+pyrrhotite).*

We now explore the individual effect of the main parameters that affect the calculated Ds, namely glass iron content, pyrrhotite stoichiometry, iron loss toward the capsule, and glass water content. If instead of 0.39 wt% FeO the glass contains 0.49 wt% (i.e. the amount of iron is allowed to increase by 1 sigma of EMPA), this increases Ds from 307 to 342. Similarly, if instead of FeS a stoichiometry of Fe_5S_6 is taken (1.2 mole of S for 1 mole of Fe), this means that 0.15 g of sulphur is locked into pyrrhotite, which decreases D_s to 202, or by 30%. Alternatively, if we assume that the Au capsule has dissolved 100 ppm Fe (corresponding to

a loss of 8 wt% of iron relative to bulk content, as observed in supra-liquidus charges by Scaillet & Macdonald (2004)), then this will increase D_s to 394. Finally, if the amount of H_2O dissolved is 4 wt% instead of 5.5 wt% (which would correspond to the possible melt H_2O content of the charges with 6 wt% sulphur), D_s decreases to 227. There is clearly a considerable uncertainty on our fluid/melt partition coefficients, yet each parameter taken in isolation affects D_s by less than 40% when allowed to vary within a reasonable range. *Our assumptions of stoichiometric pyrrhotite and fixed melt water content, if incorrect, lead to an overestimation of the calculated Ds. Conversely, other assumptions (in particular no Fe or Ca loss toward the fluid), if properly evaluated, would yield an underestimation of partition coefficients (i.e. real values are higher than the values listed in Table 2).* This is in fact the main source of uncertainty in the present work, since we have no control on the amount of dissolved fluid species other than H_2O and S. However, the work of Scaillet *et al*. (1998), using the same procedure, yielded for sulphur in silicic arc magmas partition coefficients that agree within a factor of 2 with those derived independently from remote sensing of volcanic plumes. We note in passing that this study explored the effect of CO_2 and concluded that this volatile species has no detectable effect on the partition behaviour of sulphur between fluid and melt in silicic magmas in the fO_2 range explored. We thus conclude that the partition coefficients reported here are accurate to within 50%, whilst the proportions of sulphide/sulphate are known to within 15%.

RESULTS

The experimental conditions together with run products and phase proportions are listed in Table 1. The melt compositions together with the calculated partition coefficients are listed in Table 2. Variations in melt sulphur content (S_{melt}) with fO_2 (here expressed in log units notation relative to the NiNiO solid buffer, such that NNO-1 means one log unit below NNO) are shown on Figure 1a. Also plotted is the S_{melt} of synthetic metaluminous silicic melts held under similar P and T and bulk S content (S_{bulk}) conditions (Luhr, 1990; Scaillet *et al*., 1998). The sulphur solubility of rhyolite melts is strongly dependent on their NK/A ratio, in addition to fO_2. At 800°C, under reduced conditions (< NNO), S_{melt} rises from *c.* 50 ppm in metaluminous

rhyolite to nearly 1000 ppm in strongly peralkaline rhyolite (Fig. 1a). In the two less peralkaline compositions (ND and SMN), an increase in fO_2 produces a smooth increase in S_{melt}, *which broadly conforms with observed behaviour in other silicate melt compositions (e.g. Carroll & Webster, 1994*). In contrast, in the most peralkaline composition EBU, the increase in S_{melt} peaks at around NNO+1 and then sharply decreases, so that at higher fO_2 the relative order of sulphur enrichment for the three peralkaline rhyolites is opposite to that observed below NNO. *The enhanced sulphur solubility of peralkaline rhyolites at low fO_2 is in part related to the higher iron content (Table 2), which complexes with S (Carroll & Webster, 1994), but may also be due to the greater proportion of oxygen anions in peralkaline melts relative to metaluminous varieties, since oxygen anions are believed to substitute for S (Carroll & Webster, 1994) via the following reaction:*

$$1/2\ S_2 + O^{2-} = S^{2-} + 1/2\ O_2$$

This reaction makes no assumption as to the nature of the element complexed to sulphur in the melt. It simply states that, at fixed fS_2, an increase in the activity of free oxygens will increase the amount of sulphur dissolved. Given that peralkaline melts have more free oxygens than metaluminous ones (e.g., Mysen, 1988), this could be one explanation for their enhanced sulphur solubility at low fO_2. At high fO_2, the opposite, and thus peculiar, trend displayed by EBU warrants further discussion. The above reaction predicts that an increase in fO_2 decreases the sulphur solubility, if again it is assumed that fS_2 does not change across the interval of fO_2 shown in Figure 1. However, rigorously evaluating the reason for such a trend would require us to know the exact values of intensive parameters other than fO_2, namely fS_2 and the activities of oxygen and sulphur anions in the melt, any of which is unknown in our experiments (and in almost all experimental work so far done at high P on aluminosilicate melts of geological interest). One possibility would be that our oxidized experiments with the EBU composition did not reach anhydrite saturation and thus that the anhydrite in these charges represents a quench phase and that the drop in solubility observed at high fO_2 simply reflects the fact that sulphur is being increasingly partitioned toward the fluid as fO_2 increases. We do not agree with such an interpretation because of the textural evidence given above. In addition, the

experimental conditions adopted in our study are similar to those of other experimental work aimed at defining the stability of anhydrite in silicate melts, in particular hydrous melts (e.g., Carroll & Rutherford, 1987; Luhr, 1990; Scaillet et al., 1998; Scaillet & Evans, 1999; Clemente et al., 2004), as are the criteria used to define anhydrite stability domains in magmas. In other words, if anhydrite is a quench product in our experiments, so it is in other experimental studies, in which case conclusions derived from those experiments about the stability field of anhydrite in magmas should be revised. Rather, we suggest that the trend shown by the EBU melt composition is a real feature that reflects the fundamental structural changes that occur in strongly peralkaline silicic liquids relative to metaluminous types, as noted in the introduction, and the control that fO_2 exerts upon them. By analogy with what we observe at low fO_2, we can only speculate that the increase in fO_2 dampens the role of oxygen anions in peralkaline melts, which results in a decreased S_{melt} (at fixed fS_2).

More generally, if sulphur solubility in hydrous silicic melts is a simple linear function of their iron content (at low fO_2), as conventional wisdom would predict, then there would be no reason to have the huge difference between metaluminous and peralkaline compositions that we document here (Fig. 1a). The very fact that S_{melt} increases by a factor of c. 5 between standard metaluminous rhyolitic and slightly peralkaline melts having similar iron contents, indicates that the FeO content is not the sole parameter affecting sulphur behaviour in the studied compositions, unlike in dry basaltic systems (O'Neill & Mavrogenes, 2002). This is also shown by the three series of experiments done with various amounts of sulphur, in which the melt iron content decreases whilst the amount of sulphur dissolved in the melt increases (Table 2, series EBU 7, 8 and 9). For instance, at 900°C, the melt with 969 ppm dissolved sulphur has an FeO content of 6.32 wt%, whilst that with 2254 ppm of sulphur has an FeO content of 1.52 wt%. This trend is clearly due to our procedure of adding elemental sulphur, which forces the system to crystallise FeS which in turn removes FeO from the melt. It shows, however, that the FeO content and dissolved sulphur in hydrous silicic melts are not simply correlated. In this respect, the experimental study of Clemente et al. (2004) has clearly shown that in metaluminous rhyolites, the iron control on sulphur solubility is not straightforward, and that variations in

fS_2, fH_2S and fSO_2 affect predominantly S_{melt}. This study has shown that in hydrous silicate melts, the S_{melt} can be modelled as the result of two dissolution reactions, one involving H_2S and the other SO_2, as proposed by Burnham (1979). Given the hydrous character of our experiments, it can be anticipated that the fugacities of sulphur-bearing species will exert a role, possibly a predominant one, on S_{melt} in peralkaline rhyolites as well. Direct comparison of our results with experimental studies bearing on the sulphur solubility of anydrous melts is therefore to a large extent meaningless (or of any anhydrous vs hydrous studies), since in the latter the dissolution reactions of S-bearing species cannot account for the role of H-bearing ones (i.e. H_2S), leaving aside the profound structural changes produced by the incorporation of water into silicate melts. In particular, the presence of hydrogen opens the possibility that Fe is not the element with which S preferentially complexes in silicate melts, but instead that H plays that role, as proposed by Burnham (1979), based on theoretical and experimental considerations, an hypothesis that is in agreement with the findings of Clemente et al. (2004). In other words, because both the nature and abundances of dissolving species (H_2S vs S_2 or SO_2) and the sulphur complexes in the melt (H_2S vs FeS) are likely to differ between hydrous and anhydrous melts, there is no reason to expect that results gathered from the study of sulphur in anhydrous melts can be directly applicable to hydrous melts. If this statement could be rigorously demonstrated, there would be no reasons for performing the present experimental work.

Whatever the mechanism of sulphur dissolution, our results show that at all values of fO_2, the sulphur-carrying capacity of peralkaline rhyolites is 5 to 20 times greater than their metaluminous equivalents. Increasing the temperature to 900°C increases the S_{melt} by a factor of 2, other parameters being kept equal (Fig. 2). Similarly, varying S_{bulk} from 0.5 to 6 wt% increases S_{melt} by 2-2.5 times, as a result of increasing sulphur fugacity (Fig. 2). The increase may also reflect the fact that the melt composition is changing when sulphur is added, since it removes part of the iron in solution to produce sulphide.

Variations with fO_2 in the sulphur content of fluid (S_{fluid}) over S_{melt}, or the partition coefficient D_S, are shown in Figure 1b for rhyolite melts having 1 wt% of S_{bulk}. Here again, the two less peralkaline compositions (ND, SMN) show little variation in D_S with fO_2, D_S being ≈ 270, except at around NNO+1

when anhydrite and pyrrhotite crystallise together, such as in charge ND5 which has a slightly lower D_S (Table 1). In the most peralkaline melt (EBU), however, the partition coefficient rises abruptly at fO_2 > NNO+1, behaviour similar to that found in silicic magmas from volcanic arcs (Scaillet *et al*., 1998). The reason for the limited variation in D_S in the two less peralkaline melts is that the increase in sulphur solubility with fO_2 is compensated by crystallisation of lower proportions of anhydrite at high fO_2 relative to pyrrhotite at low fO_2 (Table 1). In contrast, the increase in D_s in the most peralkaline melt is because it crystallises slightly higher proportions of sulphide at low fO_2, whilst at high fO_2 this composition does not crystallise anhydrite in higher modal amounts than ND and SMN. Because its solubility decreases beyond NNO+1, this results in an overall increase in the partition coefficient as fO_2 rises.

A comparison with experimental results obtained on a natural metaluminous dacite (Scaillet *et al*., 1998) shows that, under the same T-fO_2 conditions, a peralkaline rhyolite SMN) with bulk iron and sulphur contents similar to those in the dacite crystallises approximately 30-40 % less sulphide (Fig. 1c). Even the most peralkaline rhyolite, with 7 wt% FeO_{tot} (EBU, Table 1), crystallises less sulphide than the metaluminous dacite, which has 4.4 wt% FeO_{tot}. We interpret this as resulting from the fact that, when held at the same fO_2, the Fe^{2+}/Fe^{3+} ratio is lower in peralkaline than in metaluminous melts (Gwin & Hess, 1989; Gaillard *et al*., 2001), such that there is less Fe^{2+} available for sulphur complexation in the melt and consequently for sulphide crystallization. The lower modal proportion of sulphide in peralkaline rhyolites results in elevated fluid/melt partition coefficients, in particular for moderately peralkaline melts, even at low fO_2, differing in this respect from metaluminous melts (Scaillet *et al*., 1998). The partition coefficient steadily increases for S_{bulk} between 1 and 6 wt%, but remains broadly constant for S_{bulk} between 0.5 and 1 wt% (Fig. 3). As for the solubility trend, this reflects an increase in fS_2 perhaps coupled to a change in melt chemistry (which becomes iron-poor as the bulk sulphur content increases). At bulk sulphur content lower than 4 wt%, a rise in temperature from 800 to 900°C decreases D_S by only 10%, as a consequence of the modest increase of sulphur solubility with temperature (Fig. 3). Our results show, therefore, that any

petrogenetic process favouring the formation of peralkaline over metaluminous silicic melts will minimise the possibility of sulphur loss *via* sulphide fractionation.

The increased solubility of sulphur in peralkaline melts is consistent with the apparent scarcity of modal sulphides in peralkaline rhyolites. We are aware of three occurrences. Crisp & Spera (1987) recorded scarce pyrrhotite microphenocrysts in comendites and pantellerites of the Tejeda volcano, Gran Canaria. Mungall & Martin (1996) noted rare pyrite phenocrysts in pantellerites of the Pico Alto volcano on Terceira Island, Azores. Lowenstern *et al*. (1993) found phenocrysts of pyrrhotite and molybdenite in pantellerites and pantelleritic trachytes from Pantelleria, Italy, the occurrence of molybdenite being apparently unique in a silicate magma.

SULPHUR CONTENT OF CRUSTALLY- AND MANTLE-DERIVED RHYOLITES

General

Before using the above experimental results to constrain the atmospheric sulphur yields of rhyolites associated with flood basalts, we need to fix possible limits on the bulk sulphur contents of rhyolites, which will depend on their source region. Two end-member petrogenetic models have been proposed bearing on sulphur enrichment in magmas: crystal fractionation of basaltic magmas, e.g. the Ethiopian ignimbrites (Ayalew *et al*., 2002), and partial melting of the lower-middle continental crust (albeit with variable mantle input), e.g. the Etendeka-Paraná deposits (Bellieni *et al*., 1986; Garland *et al*., 1995; Harris & Milner, 1997; Ewart *et al*., 1998, 2004). The Ethiopian rhyolites are peralkaline, whilst the felsic magmas of the Etendeka-Paraná province are predominantly metaluminous, being in addition slightly less silicic and more K_2O-rich than those in Ethiopia. Both types of magma have high iron contents, however, which is usually attributed to low fO_2 during magma genesis (Ewart *et al*., 1998, 2004). Whatever their mode of origin, the sulphur content of silicic magmas is controlled by the source composition during partial melting and by subsequent evolutionary processes. Sulphur in a magma can reside in fluid, melt and solids, the latter being mostly sulphides under the low fO_2 thought to prevail in basalts and in the lower crust. In the following we first

consider a mantle origin (i.e., basalt fractionation) and then a crustal origin for rhyolites associated with trap sequences.

Mantle origin

Method

In basalts, sulphide stability largely dictates the possibility of generating a sulphur-rich silicic derivative since, given their high density, sulphides can easily settle out from the host magma. Thus, to produce a sulphur-rich rhyolite supposes that during fractionation the basalt does not crystallise significant amounts of sulphide. Generation of peralkaline rhyolites by fractionation of alkali basalt requires 80-90% crystallization (e.g., Barberi *et al*., 1975; Ayalew *et al*., 2002). Alkali basalts typically have bulk H_2O contents of at least 1 wt%, CO_2 contents sometimes higher than 1 wt%, and sulphur contents which can exceed 1000 ppm (Clocchiatti *et al*., 1992; Bureau *et al*., 1999; Dixon *et al*., 1997; Wallace, 2002). They evolve at $fO_2 \leq$ NNO (Dixon *et al*., 1997). We have, therefore, calculated the conditions under which alkali basalts become saturated in sulphide during crystallisation, for bulk H_2O-CO_2 contents of 1-2 wt% as inferred from studies of modern analogues (Dixon *et al.,* 1997; Gerlach *et al*., 2002; Lange, 2002), using a S_{bulk} of 0.1 wt%, and over a range of plausible redox conditions from NNO-2 to NNO+1 (Fig. 4). We also have calculated the corresponding proportions of bulk sulphur partitioned into sulphide and fluid phases (Fig. 5).

Melt compositions used. We used the basalt-rhyolite sequence of the Boina centre in the Afar rift (Barberi *et al*., 1975) as a proxy for the evolution of liquid compositions in a fractionating, mildly alkaline basalt series. Although we could have used a thermodynamical model to simulate this evolution, available models still fail to reproduce the transition from metaluminous to peralkaline melts, a feature which is critical for the understanding of sulphur behaviour, as shown below. The petrological and geochemical study of the Boina volcano concluded that the silicic magmas were derived from fractional crystallisation of transitional basalt (Barberi *et al*., 1975). Five representative compositions were used here: G485, S52, D237, D210, D224B (Barberi *et al*., 1975) (see Table 2). The degree of crystallization was determined using the K_2O content,

assuming perfectly incompatible K_2O behaviour during crystallization, a reasonable assumption except for composition D224B in which K-feldspar crystallises, and thus for which the extent of crystallization relative to the parent basalt G485 is a minimum. The following proportions of residual liquids were calculated: S52, 73%; D237, 37%; D210, 24%; D224B, 18%. This natural liquid line of descent shows that peralkaline rhyolites can be produced from basalt crystallisation after *c.* 80 wt% crystallization (Table 3, composition D224B).

Table 3. Melt compositions used in the calculations

Boina	T	melt fraction	SiO_2	Al_2O_3	FeO	MnO	MgO	CaO	Na_2O	K_2O	TiO_2	total
	H_2O	S	S max	NK/A								
	°C	wt%	wt%	wt%	wt%	wt%	wt%	wt%	wt%	wt%	wt%	wt%
	wt%	ppm	pmm									
G485	1200	100.00	46.75	13.93	10.96	0.19	9.75	10.08	2.70	0.80	2.30	97.46
	1.00	1000	1000	0.38								
S52	1088	72.73	46.03	14.80	13.67	0.12	6.04	10.36	3.00	1.10	2.50	97.62
	1.38	1375	1375	0.41								
D237	942	37.21	56.81	13.88	10.00	0.29	2.13	5.04	5.00	2.15	1.76	97.06
	2.69	2688	1290	0.76								
D210	890	24.46	59.44	15.00	7.26	0.21	1.76	4.00	4.97	3.27	1.82	97.73
	4.09	4088	850	0.78								
D224B	861	17.70	69.91	13.14	4.07	0.14	0.01	0.71	5.95	4.52	0.43	98.88
	5.65	5650	480	1.12								

Melt compositions from Barberi *et al.* (1975)
Column melt fraction gives the amount of residual melt calculated assuming that liquid G485 is parental to all others and that K_2O behaves as a perfectly incompatible element.
Column H_2O gives the H_2O content of the residual melt in the case of a basalt melt crystallising without CO_2
Column S gives the melt sulphur content if sulphur behaves as a perfectly incompatible element (no sulphide crystallisation and no fluid saturation)
Column S max gives the melt sulphur content corrected for sulphide crystallisation (aFeS = 1) for an fO_2 at NNO-2 and with no CO_2 present.
Column NK/A is the $(Na_2O+K_2O)/Al_2O_3$ molar ratio of melts.

Temperatures were calculated assuming a linear relationship between melt fraction and T, and using a liquidus of 1200°C for basalt G485 and 890°C for the rhyodacite D210 (Table 3). Clearly, such an approximation is unlikely to be valid in detail. We are, however, interested in fixing the general behaviour of C-H-O-S volatiles in a crystallising basalt, for which we need to know the approximate amount of residual melt available at each temperature in order to calculate the partitioning of each volatile species between melt and fluid using mass balance constraints and solubility laws (see below). Any departure from a linear trend will either promote or delay the attainment of volatile and sulphide saturation. This will not affect, however, the general conclusion derived from our analysis, which concerns the importance of the role of CO_2. In addition, we note that our assumption of linearity predicts a temperature of 861°C for the peralkaline rhyolite D224B, which is in reasonable agreement with available estimates for such compositions (Bizouard *et al*., 1980; Ayalew *et al*., 2002; Nekvasil *et al*., 2004). All calculations descibed below were performed for a pressure of 150 MPa since our experimental results were collected at this pressure.

Solubility and activity models. For a given initial volatile content and residual melt fraction, the amount of volatiles dissolved in the melt was calculated using the solubility models for H_2O and CO_2 of Dixon *et al*. (1995). In the absence of appropriate solution models for both H_2O and CO_2 in intermediate melt compositions, those for basalt were used. For sulphur we use the solubility model of Scaillet & Pichavant (2005). The latter is an empirical model that allows us to relate the melt sulphur content to the sulphur fugacity, for a variety of melt compositions including hydrous basalts. *This model was derived in an attempt to evaluate the behaviour of sulphur in hydrous mafic magmas*, for which there are few experimental data (apart from those of Luhr (1990)). The model has the form:

$$\log S = a\,P + b\,T + c\,\Box NNO^3 + d\,\Box NNO^2 + e\,\Box NNO\,\Box FFS + f\,\Box FFS + \Box g_i W_i \qquad (1)$$

where S is the total sulphur concentration in ppm, P the pressure in bars, T the temperature in °C, $\Box$NNO and $\Box$FFS are the referenced fO_2 and fS_2 against the Ni-NiO and Fe-FeS solid buffers respectively, W_i

represents the weight % of oxide i, and a,b,c, d, e, f and g_i are fitted parameters (Table 4) which were obtained by linear regression of the experimental data bases of Clemente *et al*. (2004), Luhr (1990) and O'Neill & Mavrogenes (2002). The summation is carried out over all major oxides, including FeO, Fe_2O_3 OH^- and H_2O. This third order polynomial function is necessary to reproduce the inverted bell-shaped pattern of sulphur solubility in silicate melts (e.g., Carroll & Webster, 1994; Clemente *et al*., 2004), whilst the crossed fO_2-fS_2 term is needed to take into account the effect of varying fS_2 on the relationship between fO_2 and S in melt (Clemente *et al*. 2004).

Table 4 : regression coefficients for the empirical model of sulphur solubility

P	7.28E-06
NNO^3	0.00488128
NNO^2	0.0818873
NNOFFS	-0.0224068
T	0.00084107
FFS	0.22801636
SiO_2	-0.012467
Al_2O_3	-0.0015766
Fe_2O_3	0.37362348
FeO	0.0674383
MgO	0.01121929
CaO	0.02000831
Na_2O	0.05644745
K_2O	-0.0248037
TiO_2	0.00672403
H_2O	0.06868295
OH	0.05778453

From Scaillet & Pichavant (2005)

This model encompasses a large SiO_2 range (35-80 wt%), and reproduces measured fS_2 within an average of 0.65 log unit, over more than 15 log units when normalised to the FFS solid buffer. Finally, note that the model of Scaillet & Pichavant (2005) is calibrated only for metaluminous compositions, which implies that sulphur solubilities of intermediate or silicic peralkaline compositions corresponding to any given fS_2 are underestimated by this model and thus that sulphide activities calculated here for those melts are overestimated (see below).

For any fO_2 and fS_2, the activity of FeS in the melt was calculated from the following equilibrium, using thermodynamic data from O'Neill & Mavrogenes (2002):

$$FeS + 1/2\ O_2 \text{ <--> } FeO + 1/2\ S_2 \qquad (2)$$

The activity of FeO in the melt was calculated by determining the Fe^{2+}/Fe^{3+} ratio of the melt using the Kress & Carmichael (1991) method and an activity coefficient for FeO of 1.4 (O'Neill & Mavrogenes, 2002). For any melt in which the calculated FeS activity was found to exceed 1, the melt sulphur content was fixed to that corresponding to an aFeS=1, and the excess sulphur was converted to sulphide (we thus neglect the role of additional elements such as Ni or Cu which could promote early saturation in sulphide).

The fluid phase composition was calculated using a Modified Redlich-Kwong type equation of state (MRK), using as input parameters fH_2O, fCO_2 and fS_2. It must be stressed that, regardless of our current knowledge or body of experimental constraints on the sulphur content of fluids in magmas, the sulphur content of a fluid coexisting with silicate melts can be calculated using a thermodynamic approach, provided that appropriate solubility laws exist for the main volatiles species. This stems from the fact that in the C-O-H-S system, once fH_2O, fCO_2 and fS_2 are fixed (at P and T), the fugacities of all other volatile species are fixed as well (Holloway, 1987; Scaillet & Pichavant, 2003; 2004). In other words, the composition of the fluid is uniquely defined, including its sulphur content. This allows us to compute the partition coefficients of sulphur between fluid and melt, since the melt sulphur content is fixed by fS_2 (and fO_2). The accuracy of such an approach relies, among other things, on our knowledge of the thermodynamic properties of C-O-H-S fluids which appear to be reasonably well known (e.g., Shi, 1992), at least in the low pressure range (<1000 MPa). Using this approach, Scaillet & Pichavant (2003) showed that there was a good overall agreement between calculated and measured fluid compositions for silicic arc magmas. The same method has been applied to active basaltic volcanoes (Scaillet & Pichavant, 2005), for which remote sensing of volcanic gases can be used to constrain the gas chemistry at depth. In this case too, generally good agreement is observed (Scaillet & Pichavant, 2005). Therefore, although we recognise that the current experimental data base on the sulphur content of fluids of mafic magmas is almost non-existent, this gap can be partly circumvented by

using a thermodynamic approach which, when compared to independent estimates, appears to retrieve the correct order of magnitude in terms of the sulphur content of magmatic fluids.

Procedure. For any given initial H_2O, CO_2 and S contents, the equilibrium distribution of those volatiles between melt, fluid and sulphide was calculated via an iterative procedure by finding the fugacities that satisfy the following two sets of conditions: First, the condition of chemical equilibrium:

$$fH_2O_{melt} = fH_2O_{fluid}, \quad (3)$$

$$fCO_{2melt} = fCO_{2fluid}, \quad (4)$$

$$fS_{2melt} = fS_{2fluid} \quad (5)$$

Second, the mass balance constraints:

$$H_2O_{total} = H_2O_{melt}+H_2O_{fluid} \quad (6)$$

$$CO_{2total} = CO_{2melt}+CO_{2fluid} \quad (7)$$

$$S_{total} = S_{melt}+S_{fluid}+S_{sulphide} \quad (8)$$

The mass balance equations also take into account the amounts of C, S and H in other species such as H_2S, SO_2, CO and CH_4. In the H_2O-only case, with a bulk H_2O content of 1 wt%, we considered that the crystallising basalt does not reach fluid-saturated conditions since the H_2O content of the residual melt reached after 82% crystallisation is 5.65 wt% (Table 3), that is on the verge of H_2O saturation of rhyolitic melts at 150 MPa **(**e.g., Zhang, 1999**).** In this case, the sulphur was partitioned between melt and sulphide only.

Consider, as an example of the calculation procedure, the case of a basalt carrying only H_2O and sulphur crystallising at an fO_2 of NNO-2. *At 890°C, the basalt has 24.46 wt% residual liquid with a composition of D210 (Table 3). If sulphur had a perfectly compatible behaviour (bulk S of 1000 ppm), then the melt composition D210 would have 4088 ppm of dissolved sulphur (1000/0.2446). Using the model of Scaillet & Pichavant (2005), this amount of dissolved sulphur would correspond to an fS_2 of 0.035 MPa, or to an aFeS=18 when calculated using equilibrium (2) and the assumptions given above. Clearly, there is too*

much sulphur in solution and some of it must be withdrawn in order to decrease the aFeS to unity, since by definition the activity of FeS cannot increase beyond 1 (for appropriate standard states for solids and liquids at P and T). The next step is thus to remove the excess sulphur in solution in the melt until the calculated fS_2 corresponds to an aFeS=1, and convert that excess sulphur into immiscible/solid sulphide (considering also the constraints set out in equations (3) to (8)). For that specific case, using equation (1), we calculate that saturation of melt composition D210 with sulphide (aFeS=1, because we perform an equilibrium calculation, aFeS in the silicate liquid is equal to that in the sulphide) is achieved when $fS_2 = 10^{-4}$ MPa at 890°C and NNO-2, which corresponds to a melt sulphur content of 850 ppm. In other words, it means that of the 1000 ppm sulphur dissolved in the molten basalt at 1200°C, 208 ppm (850x0.2446) are dissolved in the residual melt at 890°C, the remainder (792 ppm = 1000-208) being locked up in sulphide, since under these conditions no fluid is present (Table 3, the melt water content is below the saturation value of an andesitic melt at 150 MPa (Burnham, 1979)). The introduction of CO_2 into the system promotes early fluid saturation and thus the sulphur content of melt at 890°C (i.e., when there is only 24.46 wt% residual melt) must be lower than when only H_2O is present. For instance, implementing the example above with addition of CO_2, that is, a basalt with 1 wt% H_2O and 1 wt% CO_2 at NNO-2, we calculate that at 890°C the sulphur content of the residual melt is 635 ppm. Finally, as noted above, peralkaline melts dissolve more sulphur than metaluminous types, so our calculated sulphide proportions should be considered maxima for the most fractionated melt (D224B, Table 3). Assuming, on the basis of our experimental results, that the peralkaline melt D224B dissolves 5 times more sulphur than that calculated by the model of Scaillet & Pichavant (2004), or 4250 ppm, then it follows that such compositions would be barely saturated at NNO-2, the proportion of sulphide being low. This implies that the amounts of CO_2 needed to scavenge the sulphur toward the fluid, which under our P-T conditions is calculated to be 2 wt% (see below), must be considered maximum values where peralkaline derivatives are produced.

Results

The results of our calculations are shown on Figures 4, 5 and 6. We have considered three cases corresponding to different bulk volatile contents: case (1), 1 wt% H_2O and 1000 ppm sulphur, case (2) 1 wt% H_2O, 1 wt.% CO_2 and 1000 ppm sulphur, and case (3) 2 wt% H_2O, 2 wt% CO_2 and 1000 ppm sulphur. Figure 4a shows the evolution of aFeS of a basalt with degree of crystallization, calculated at four different fO_2. An H_2O-bearing (1 wt%) but CO_2-free alkali basalt crystallising at or above NNO-1 is sulphide-saturated after *c*. 60% of crystallization. At NNO-2, saturation in sulphide is slightly delayed, to 70% crystallization. Figure 5a shows the evolution of the proportion of bulk sulphur sequestered in sulphide with degree of crystallization, corresponding to the calculations shown in Fig. 4a. By the time the residual melt is peralkaline (20-30% liquid, see Table 2), it can be seen that 90 wt% of S_{bulk} is locked up in sulphide (Fig. 5a). Further crystallisation results in massive sulphide precipitation; after 82% crystallisation more than 80 wt% of S_{bulk} is locked up in sulphide. The calculations corresponding to case (2) illustrate the role of CO_2. When this volatile is introduced, the sulphur behaviour is dramatically altered because fluid saturation occurs at an early stage, owing to the low solubility of CO_2 in silicate melts (e.g., Dixon *et al*., 1995) and chemical equilibrium demands that sulphur is also partitioned into the fluid, thus lowering S_{melt} and the activity of sulphide. With a bulk CO_2 content of 1 wt% and 1 wt% H_2O (case 2), similar to the bulk content inferred for Kilauean or Etnean basalts (Clocchiatti *et al*., 1992; Gerlach *et al*., 2002), the calculations show that sulphide saturation is slightly delayed compared to the H_2O-only case (Fig. 4). However, the main difference relative to the CO_2-free situation (case 1) is that after 80% crystallisation, at least 60 % of S_{bulk} is in the fluid phase, whatever the prevailing redox conditions, rising to 90% for fO_2 = NNO+1 (Fig. 5b). Finally, case (3) shows that at fO_2 = NNO-2, for initial CO_2 and H_2O contents of 2 wt% each, a crystallising alkali basalt remains below sulphide saturation, even after 80% crystallization when derivative liquids are rhyolitic (Fig. 6). Under these conditions 95% of S_{bulk} is hosted by the fluid, even after 80 wt% of crystallization (Fig. 5b).

We stress that such elevated bulk volatile contents have been inferred for some alkali basalts (Dixon *et al.,* 1997), including those in flood sequences (Lange, 2002). In addition, recent experimental data on the generation of silica-saturated alkalic suites from alkali basalts suggests that the latter contain at least 0.5 wt% H_2O, and possibly up to 2 wt% (Nekvasil *et al*., 2004), which reinforces the view that trap basalts may be considerably richer in fluids than those at mid-ocean ridges. The above calculations show that, provided they are CO_2- and H_2O- rich, basaltic magmas can readily produce sulphur-rich derivatives, regardless of the imposed redox conditions. The amount of CO_2 appears to be the key parameter, since it triggers early volatile exsolution which prevents sulphide precipitation. Without CO_2, fO_2 exerts a prime control on the amount of sulphide crystallisation in basalt with a certain initial sulphur content. A reduced CO_2-poor basaltic magma will yield silicic derivatives which are sulphur-poor owing to extensive sulphide precipitation, whilst a basalt crystallising at or above NNO+1, as in arc settings, may give rise to sulphur-rich silicic magmas (Scaillet & Pichavant, 2003; Scaillet *et al*., 2003). The presence of CO_2 in large amounts significantly reduces this fO_2 control. If alkali basalts are CO_2-rich, they can release >90% of their S_{bulk} during crystallisation. After the stage of rhyolite production, the ultimate fate of sulphur will be dictated by the composition of the melt, particularly its NK/A ratio (in addition to fO_2, Scaillet *et al.,* 1998). As our experimental data show, metaluminous felsic magmas can carry less sulphur in solution than peralkaline types, especially at low fO_2. We conclude that if alkali basalt fractionation produces peralkaline rhyolites, these may well be sulphur-rich, concentrating a significant proportion of the original sulphur content of the parent magma.

Crustal origin

Method

To constrain the sulphur content of silicic melts produced by partial melting of the lower crust, we have calculated the sulphur contents of (1) anatectic melts and (2) metamorphic fluids in the amphibolite-granulite facies. The sulphur content of crustal melts can be calculated using the solubility model for

sulphur of metaluminous rhyolites derived by Clemente et al. (2004), since dehydration melting of mid- to lower- crustal lithologies produces dominantly metaluminous or peraluminous silicic melts (Clemens & Vielzeuf, 1987). The ambient fS_2 conditions during crustal melting are likely to be controlled by sulphide equilibria, such as pyrite-pyrrhotite (Poulson & Ohmoto, 1989). Under lower crustal conditions, this equilibrium fixes fS_2 at c. 0.1 MPa (Shi, 1992). Therefore, the calculations were performed by fixing fO_2, fH_2O and fS_2, at fO_2 ranging from NNO-2 to NNO+2, which are likely to encompass redox conditions in the lower crust. We explored specifically the sulphur solubility for three different melt H_2O contents, 1, 2 and 3 wt%, since we are interested in anatectic melts that are relatively dry (see below). At any fO_2, fixing the melt water content fixes fH_2O (using the thermodynamic model of H_2O solubility of Zhang, 1999) and thus fH_2. Given that we set fS_2 as constant, this allows us to calculate fSO_2 and fH_2S which are then used as input parameters in the thermodynamic model of Clemente et al. (2004), from which theamount of sulphur dissolved in the rhyolitic melt arising from the additive contributions of H_2S and SO_2 species is derived. For metamorphic fluids, we have calculated the sulphur content of a C-O-H-S fluid phase likely to be present in the mid to lower crust, assuming again an fS_2 controlled by the pyrrhotite-pyrite equilibrium (i.e. fS_2 =0.1 MPa). To this end we have used the MRK equation of state introduced above and explored various fO_2 conditions likely to encompass crustal redox states as well as various water activities (expressed as XH_2O in figure 7b). As detailed for the basalt above, we fix fO_2, fH_2O and fS_2 as input parameters in order to calculate the fluid phase composition. The temperature at which we calculate the composition of metamorphic fluids, 800°C, is lower than that considered for anatexis (1000°C) since we are interested in the amount of sulphur that can be transported in metamorphic fluids prior to widespread partial melting. In summary, as for the crystallization of basalt detailed above, we have calculated the equilibrium sulphur contents of a fluid and rhyolitic melt, under P-T-fO_2-fS_2 conditions considered likely to prevail in the lower crust. By comparing the sulphur contents of crustally derived metaluminous melts with those of metamorphic fluids, we aim to constrain the overall behaviour of sulphur in hot mid to lower crust flushed by melts or fluids.

Results

Figure 7a shows that the sulphur content of silicic melts for melt water contents ≤3 wt% and fO_2 in the range NNO-2 to NNO+1, all calculated for an fS_2 of 0.1 MPa, does not exceed 200 ppm. In contrast, the sulphur content of metamorphic fluids under similar P-T-fO_2 conditions is strongly dependent on fO_2 and water fugacity, and it reaches several wt%, except from nearly dry conditions (Table 7b. From Figure 7a, we conclude that silicic melts produced in the mid to lower crust are unlikely to reach values of S_{melt}, and thus S_{bulk} if extracted from their source, much higher than 200 ppm. This value should be considered as a maximum for the following reasons: firstly the sulphur content of the lower crust is estimated to be c. 400 ppm (Wedepohl, 1995), which indicates a rather small sulphur buffering capacity during melting. Secondly, crustal melts associated with flood basalts record temperatures in the range 900°C to >1100°C (Bellieni et al., 1985; Harris & Erlank, 1992; Garland et al., 1995; Harris & Milner, 1997; Ewart et al., 1998, 2004), which has led to the suggestion that such felsic magmas were produced from previously dehydrated crust (Kilpatrick & Ellis, 1992). The dehydration event could have involved fluids and/or melts but in any case, in view of the sulphur content of such melts/fluids (Fig. 7), such a dehydration event is likely to have removed most of the sulphur budget of the crustal protolith. Subsequent partial melting of dehydrated lower crust is thus unlikely to produce sulphur rich magmas.

Summary

We thus envisage basalt-derived rhyolites as magmas that can potentially carry several thousands of ppm of sulphur, either dissolved in the melt or in a separate fluid phase, with only minor amounts trapped in coexisting sulphide, especially when they are peralkaline. In contrast, the sulphur content of crustally-derived melts is calculated to be less than 200 ppm, especially if formed from dehydrated lower crust.

DISCUSSION

Sulphur yields of Ethiopian, Deccan and Paraná-Etendeka silicic rocks

We first address the Ethiopian sequences for which the pre-eruptive sulphur contents are reasonably well known, melt inclusion analyses having yielded S_{melt} in the range 400-500 ppm (Ayalew *et al*., 2002). The NK/A ratios of Ethiopian rhyolites range from *c.* 1 to 1.4, which corresponds to the two less peralkaline samples used in our experiments. Pre-eruptive temperatures have been estimated at 740-900°C. The pre-eruptive water content is not well known but similar rhyolites from the Ethiopian rift had melt H_2O contents of 4-8 wt% (Webster *et al*., 1993). Redox states are poorly constrained, yet such rhyolites are generally inferred to evolve at fO_2 < NNO (e.g., Mahood, 1984 ; Scaillet & Macdonald, 2001 ; White et al., 2005). High water contents are consistent with 80-90 % crystallization of parent alkali basalts (Ayalew *et al*., 2002) with an initial bulk H_2O content of 1 wt%. If fractionation occurs at shallow levels (<200 MPa), then H_2O saturation of the liquid will occur after 80% crystallization if no CO_2 is present, or earlier with CO_2. At 150 MPa, a basalt with 1 wt% H_2O initially can yield a rhyolite magma with 5-6 wt% dissolved H_2O coexisting with 4-6 wt% fluid, provided that both melt and fluid have left their source. The amount of free fluid might well be larger, however, since this estimate does not include CO_2. Using a conservative bulk initial S content of 1000 ppm for the parental basalt, then rhyolite produced after 90% crystallisation will potentially carry up to 1 wt% sulphur. With this S_{bulk} and at fO_2 < NNO, moderately peralkaline rhyolites dissolve 200-300 ppm sulphur at 800°C, or 400-500 ppm at 900°C (Fig. 1a). The sulphur content of the coexisting fluid phase ranges between 6 and 10 wt% (Table 1). The fact that the sulphur contents of both natural and experimental melts compare closely indicates that the chosen experimental conditions broadly correspond to those of magma storage before eruption.

We can now evaluate the potential sulphur delivery to the atmosphere by the Ethiopian rhyolites, whose estimated volume is 60,000 km^3 (dense rock equivalent or DRE, Ayalew *et al*., 2002). Assuming that

such magmas coexisted with 5 wt% fluid, the bulk sulphur erupted ranges from $4.3x10^{17}$ g for an S_{fluid} of 6 wt% to $7.3x10^{17}$g for S_{fluid} = 10 wt%. These estimates are one order of magnitude higher than previous figures (Ayalew *et al*., 2002), basically because the fluid contribution, in which 90% of the sulphur in melt+fluid is stored, has been taken into account.

Evaluation of the sulphur yield of the Etendeka-Paraná silicic eruptives is somewhat simpler. The magmas have been inferred to be nearly dry, on the basis of elevated temperature estimates and lack of hydrous phenocrysts (Ewart *et al*., 1998, 2004), indicating that they were probably not fluid-saturated at depth. This essentially restricts their atmospheric sulphur yield from melt degassing during ascent to the surface. Using an estimated volume of 20,000 km^3 (Harris & Milner, 1997) and a conservative pre-eruptive S_{melt} content of 100 ppm, we calculate that these silicic magmas were capable of delivering no more than $4.6x10^{15}$ g of sulphur to the atmosphere when fully degassed, or almost two orders of magnitude less than the Ethiopian contribution, for comparable volumes of erupted magmas.

The Deccan flood basalts are associated with minor amounts of silicic rocks, estimated to reach 500 km^3 (Lightfoot *et al*., 1987). Although a partial melting origin from basalt protoliths has been advocated (Lightfoot *et al*., 1987), the Deccan rhyolites share most of the major element characteristics of the Ethiopian sequences. In particular, they are strongly peralkaline which is marked, *inter alia*, by very high Zr concentrations compared to metaluminous rhyolites. The high solubility of Zr in peralkaline rhyolites is a well established feature (e.g. Watson, 1979; Linnen & Keppler, 2002; Scaillet & Macdonald, 2003)

Assuming that the sulphur yield of Deccan rhyolites scales with that of the Ethiopian rhyolites, between $3.6x10^{15}$ and $6.1x10^{15}$ g of sulphur could have been emitted. However, pre-erosional volumes of silicic magmas may have been much larger than the current outcrop (Bryan *et al*., 2002). Javoy & Courtillot (1989), for example, have suggested that a short term variation in the seawater $^{87}Sr/^{86}Sr$ ratio at the Cretaceous-Tertiary boundary could have been due to intense silicic volcanism related to Deccan basalts, and estimated their volume to about 50,000 km^3, which is comparable to Ethiopian rhyolites. If it is assumed that Deccan basalts were somehow able to produce peralkaline derivatives at the same yield as in

Ethiopia (thereby producing roughly twice the Ethiopian silicic volumes), the Deccan rhyolites could have produced $0.9x10^{18}$-$1.5x10^{18}$g of S, comparable to the estimate for the basalt emissions alone (Wignall, 2001).

Environmental consequences

The most common explanation for the formation of Large Igneous Provinces, including continental flood sequences (Coffin & Eldholm, 1994), is that they result from periodic mantle-core instability that generates hot mantle plumes which *via* adiabatic melting lead to a widespread but short-lived melting episode when the plume reaches shallow mantle levels. Much recent interest on flood activity has stemmed from the recognition that there is a strong correlation between periods of major basalt eruption and worldwide environmental crises such as mass extinctions and oceanic anoxic events (e.g. Courtillot & Renne, 2003). A causal link between those two events has therefore been claimed (e.g. Vogt, 1972; Morgan, 1981; Courtillot, 1999; Rampino & Self, 2000; Courtillot & Renne, 2003). Establishing whether such a causal link indeed exists rests primarily on (1) obtaining precise timing constraints of the geological events and (2) evaluating the volatile contributions of flood events to the atmosphere, since it is thought that massive emissions of climate-sensitive volatile species are a major contributing factor to global climate change. In particular, the volcanic hypothesis of mass extinctions hinges critically on the injection of massive amounts of volcanic sulphur into the atmosphere, which, in addition to CO_2, is one of the controlling factors of climate variability (Robock, 2000).

Whilst decisive progress has been made in recent years with respect to the effects of CO_2 (see Courtillot & Renne, 2003), our ability to analyse the role of S emissions has been less successful. Sulphur emissions of past flood events have been largely evaluated using simple scaling arguments which assume that present-day magmas have a sulphur content comparable to those erupted during flood eruptions, *basically because, in most instances, it is the only approach that can be applied, especially when the events considered are old, in which case critical data needed to assess sulphur yield, in particular glassy melt*

inclusions, are lacking. For instance, the 1783-1784 Laki fissure eruption on Iceland and its climate aftermath (Métrich *et al*., 1991; Thordarson *et al*., 1996; Thordarson & Self, 2003) is often taken as a representative, yet smaller scale, scenario for the environmental consequences of flood basalt emissions (e.g. Eldholm & Thomas, 1993; Stone, 2004). *For silicic compositions*, it is well established, however, that such an approach can lead to dramatic under- or over-estimations of the sulphur content of the original magmas (Scaillet *et al*., 1998). As shown for andesite and rhyolite in arc settings, the sulphur content at the time of eruption can differ by orders of magnitude between magmas having similar compositions but different redox states (Scaillet *et al*., 1998). *The present study illustrates an additional factor to be considered when assessing the sulphur yield of silicic magmas, that is their Na+K/Al ratio. For mafic magmas,* given the vagaries of melt generation, storage and evolution in the mantle, there is no *a priori* reason to ascribe to flood basalts a common value for their sulphur content, *and it remains to be established whether the scaling–up procedure yields correct numbers, although in most cases this is perhaps the only approach that we can use.* Our analysis shows that the ultimate fate of sulphur in basalt will be heavily dependent on the bulk CO_2 content of the system. *It shows, though, that under near-liquidus conditions, most of the sulphur remains dissolved in the melt, even when the basalt coexists with considerable amounts of H_2O and CO_2. For instance, on Fig. 5b the case of a basalt at NNO-2 with 2 wt% H_2O+CO_2 shows that at near liquidus conditions (i.e. more than 80% melt) the magma has less than 10% of its sulphur hosted by the fluid, the remaining being dissolved in the melt since no sulphide is present under such conditions (i.e., aFeS<1, Fig. 6). This implies that, for eruptions involving crystal-poor basaltic magmas, estimates of atmospheric sulphur yields relying on the difference in sulphur contents between melt inclusions and matrix glasses (i.e. estimates which ignore the fluid contribution) will get figures which are close to real values, as illustrated for recent basaltic eruptions for which independent estimates of sulphur yields using remote sensing methods are available (Sharma et al., 2004).*

In addition to these evaluation problems, the causal link between volcanoes and climate has been criticized on several grounds (Wignall, 2001), and in particular on the fact that volatiles emitted during

effusive basaltic eruptions are unable to reach the upper atmosphere. Although theoretical studies have shown that flood activity can lead to stratospheric loading of magmatic volatiles (Woods, 1993), the effusive nature of basalt is still considered as a major shortcoming of the flood-driven mass extinction hypothesis (Wignall, 2001). This is unlike the case for their silicic counterparts, which, owing to their explosive nature, are able to result in major stratospheric sulphur loading with regional to hemispheric dispersion (Rampino & Self, 1992). However, all studies aimed at evaluating such an hypothesis have exclusively considered flood activity and its attendant environmental impact to be due to basalt emissions and have ignored the role of associated silicic magmas. In fact, the generation of copious amounts of silicic magmas by melting of continental crust should be an expected consequence of plume impingment at the base of the continental crust (Javoy & Courtillot, 1989). *Recent detailed thermal modelling studies have indeed confirmed that widespread production of felsic magmas, either via crystal fractionation of basalt magma or via partial melting of the surrounding crust, is an inescapable by-product of basalt intrusion in the lower crust (Annen & Sparks, 2002; Annen et al., 2006).* Thus there exists the possibility that the overall volcanic events had a global, long lasting, impact on climate through their silicic emissions. In this paper, we have attempted to evaluate the contribution of the silicic end- members of flood activity to atmospheric sulphur release and have shown that, in some cases at least, it may have been volumetrically as large as the associated basalts.

The Ethiopian Traps flood sequences coincided with a worldwide oceanic cooling event (Rochette *et al*., 1998; Touchard *et al*., 2003), whilst the Paraná-Etendeka eruptives are the only flood sequence not synchronous with a documented major environmental change or mass extinction event (Courtillot & Renne, 2003). Our results offer one explanation, namely the contrasted sulphur yields of the silicic activity. Besides this parameter, factors controlling eruption dynamics may also have played an important role. Water is critical in producing the high and sustained eruptive columns (Sparks *et al*., 1997) which are required for global dispersion of volcanic volatiles via injection of magmatic volatiles into the stratosphere. The Ethiopian rhyolitic magmas were possibly cooler and richer in water than the Etendeka-Paraná rhyolites. We thus speculate that in the former case, the conditions of explosive eruption were easily achieved and the

recent discovery of ash layers at several places in the Indian Ocean having the correct age and composition (Touchard *et al*., 2003) is circumstantial evidence that at least part of the Ethiopian rhyolites were emitted during highly energetic eruptions. In contrast, the high to very high pre-eruption temperatures inferred for the Etendaka-Paraná silicic deposits point to rather low magma viscosity which, together with their anhydrous character, could have favoured a mostly effusive regime (Kirstein *et al*., 2001), with much less potential for hemispheric stratospheric loading of its volatiles. *Lastly, the recent thermal simulation results of Annen et al. (2006) of basalt intrusion at the base of the crust show that rhyolite production via fractionation of basalt occurs before that due to partial melting of the crust. In detail, the time interval between the onset of basalt intrusion (and emission) and the widespread production of silicic magmas is dependent on a number of factors (depth of intrusion, fertility of the crust, emplacement rate of basalt, ambient geotherm) and varies between 0.02 Myr and several Myr in the case of slowly intruded mafic magmas. Yet, results show that rhyolite floods originated via partial melting will be erupted later than those produced by basalt fractionation. In addition to this incubation time, modelling shows clearly that the basalt fractionation mechanism for rhyolite generation has a higher productivity than partial melting of the crust. For instance, intrusion at 30 km depth of basalts with 2.5 wt% H_2O, with 50 m thick sills injected every 10 kyr, is able to produce c. 18% of silicic melts via fractionation (18% relative to the total volume of intruded basalt) 500 000 years after the onset of the process, whilst, within the same time interval, partial melting of overlying amphibolite crust is able to yield only 3 % of silicic melt (Fig. 10 of Annen et al., 2006). The above lines of evidence (higher sulphur yield and explosivity, shorter incubation time and greater productivity) all combine to suggest that flood rhyolites formed via basalt fractionation are more likely to have a greater environmental impact than those due to partial melting of the crust.*

The foregoing discussion suggests that magmatic traps associated with silicic emissions can be tentatively classified into two main groups: those having produced dominantly metaluminous magmas and those associated with peralkaline rhyolites *sensu lato*. Given the generally poor preservation of silicic flood sequences (Bryan *et al*., 2002), we can only speculate at this stage as to their classification. Silicic traps

associated with the Karoo basalts are similar to those of Etendeka-Paraná (Harris & Erlank, 1992) and are associated with an extinction event which is minor considering the volume of erupted basalt (Wignall, 2001). On the other hand, the Emeishan Trap basalts, which are broadly coeval with the massive Permo-Triassic mass extinction, are associated with scarce silicic eruptives of possible peralkaline affinity (Xu *et al*., 2001). Given that most provinces display both metaluminous and peralkaline felsic rocks (Bryan *et al*., 2002), it is also important to evaluate the proportions of each magma type.

Finally, we note that melting of crust in back-arc settings may be a particularly favourable locus for the generation of voluminous amounts of silicic magmas with only minor basalts, e.g. the Sierra Madre Occidental in western Mexico and Chon Aike in South America (Bryan *et al*., 2002). Such rhyolites may have formed by crustal melting following protracted subduction zone magmatism, the latter having extensively hydrated the lower crust. Such a process could conceivably increase the sulphur content of the lower crust, given the high sulphur contents of arc magmas (Scaillet *et al*., 2003). Melting of such protoliths may produce silicic melts rich in water and perhaps in sulphur.

CONCLUSIONS

Our study shows that rhyolite magmas may act as an important conveyor of mantle sulphur toward the atmosphere, especially when their parental basalts are rich in volatiles, particularly CO_2. We do not dismiss the important role played by the basaltic component in terms of volatile output. Our study simply suggests that, in addition to volumes of erupted basalt and the duration of peak activity, the environmental consequences of flood magmatism may or may not be greatly enhanced by their silicic component. When voluminous peralkaline derivatives are produced, their explosive emission may give the coup de grâce to the worldwide changes triggered by early basaltic emissions. We note that an alternative scenario to the conventional core-mantle origin of flood sequences is that trap basalts are rooted in an anomalously volatile-rich sublithospheric mantle (Anderson, 1994). Although still scanty, available evidence suggests that trap basalts are indeed richer in volatiles than those erupted at oceanic ridges (e.g., Lange, 2002; Rodriguez

Durand & Sen, 2004). Given the generally poor preservation of silicic members, in particular in old sequences, we suggest that future studies aimed at evaluating the environmental consequences of flood activity focus on the evaluation of the volatile contents of basalts. In addition, a better petrogenetic understanding of the processes leading to peralkaline derivatives in bimodal suites is highly desirable.

ACKNOWLEDGEMENTS

Ongoing discussions with Michel Pichavant and John Mavrogenes helped our understanding of important features related to the behaviour of sulphur in magmas. Thorough and helpful reviews were provided by Jim Webster, Malcolm Rutherford and an anonymous reviewer. The careful editorial handling of Marjorie Wilson and Alastair Lumsden is gratefully acknowledged.

References

Anderson, D.L. (1994). The sublithospheric mantle as the source of continental flood basalts ; the case against the continental lithosphere and plume head reservoirs. *Earth and Planetary Science Letters* **123**, 269-280.

Annen, C. & Sparks, R.J.S. (2002). Effects of repetitive emplacement of basaltic intrusion on thermal evolution and melt generation in the crust. *Earth and Planetary Science Letters* **203**, 937-955.

Annen, C. Blundy, J. & Sparks, R.J.S. (2006). The genesis of intermediate and silicic magmas in deep crustal hot zones. *Journal of Petrology*, in press.

Ayalew, D., Barbey, P., Marty, B., Reisberg, L., Yirgu, G. & Pik, R. (2002). Source, genesis, and timing of giant ignimbrite deposits associated with Ethiopian continental flood basalts. *Geochimica et Cosmochimica Acta* **66**, 1429-1448 .

Bailey, D.K. & Schairer, J.F. (1966). The system Na_2O-Al_2O_3-Fe_2O_3-SiO_2 at 1 atmosphere, and the petrogenesis of alkaline rocks. *Journal of Petrology* **7**, 114-170

Baker, D.R. & Vaillancourt, J. (1995). The low viscosities of F+H_2O-bearing granitic melts and implications for melt extraction and transport. *Earth and Planetary Science Letters* **132**, 199-211.

Barberi, F., Ferrara, G., Santacroce, R., Treuil, M. & Varet, J. (1975). A transitional basalt-pantellerite sequence of fractional crystallisation, the Boina Centre (Afar rift, Ethiopia). *Journal of Petrology* **16**, 22-56.

Bellieni, G., Comin-Chiaramonti, P., Marques, L.S., Melfi, A.J., Nardy, A.J.R., Papatrechas, C., Piccirillo, E.M., Roisenberg, A. & Stolfa, D. (1986). Petrogenetic aspects of acid and basaltic lavas from the Paraná plateau (Brazil) : geological, mineralogical and petrochemical relationships. *Journal of Petrology* **27**, 915-944.

Bizouard, H., Barberi, F. & Varet, J. (1980). Mineralogy and petrology of Erta Ale and Boina volcanic series, Afar rift, Ethiopia. *Journal of Petrology* **21**, 401-436

Bryan, S.E., Riley, T.R., Jerram, D.A., Stephens, C.J. & Leat, P.T. (2002). Silicic volcanism: an underevaluated component of large igneous provinces and volcanic rifted margins. In: Menzies, M.A., Klemperer, S.J., Ebinger, C.J. & Baker, J. (eds) *Volcanic rifted margins. Geological Society America Special Paper* **362**, 97-118.

Bureau, H. Métrich, N., Semet, M.P. & Staudacher, T. (1999). Fluid-magma decoupling in a hot spot volcano. *Geophysical Research Letters* **26**, 3501-3504.

Burnham, C.W. (1979). The importance of volatile constituents. In H.S. Yoder (ed.) *The evolution of the igneous rocks, fiftieth anniversary perspectives*. Princeton Univ. Press, New Jersey, 439-482.

Burnham, C.W., Holloway, J. R. & Davis, N. F., 1969. Thermodynamic properties of water to 1000°C and 10000 bar. *Geological Society of America Special Paper* **132**.

Carroll, M.C. & Rutherford, M.J. (1985). Sulfide and sulfate saturation in hydrous silicate melts. *Journal of Geophysical Research* **90** (supp.), C601-C612.

Carroll, M.R. & Webster, J.D. (1994). Solubilities of sulfur, noble gases, nitrogen, chlorine, and fluorine in magmas. In: Carroll, M.R. & Holloway, J.R. (eds) *Volatiles in Magmas. Reviews in Mineralogy* **30**, 231-279.

Chabot, N.L. (2004). Sulfur contents of the parental metallic cores of magmatic iron meteorites. *Geochimica et Cosmochimica Acta* **68**, 3607-3618.

Clemens, J. & Vielzeuf, D. (1987). Constraints on melting and magma production in the crust. *Earth and Planetary Science Letters* **86**, 287-306.

Clemente, B., Scaillet,B. & Pichavant, M. (2004). The solubility of sulphur in rhyolitic melts. *Journal of Petrology* **45**, 2171-2196.

Clocchiatti, R., A., Weisz, J., Mosbah, M. & Tanguy, J.C. (1992). Coexistence de verres alcalins et tholéiitiques saturés en CO_2 dans les olivines des hyaloclastites d'Aci Castello (Etna, Sicile, Italie). Arguments en faveur d'un manteau anormal et d'un réservoir profond, *Acta Vulcanologica* **2**, 161-173.

Coffin, M.F. & Eldholm, O. (1994). Large igneous provinces: crustal structure, dimensions, and external consequences. *Reviews of Geophysics* **32**, 1-36.

Costa , F., Scaillet, B. & Pichavant, M. (2004). Petrological and experimental constraints on the pre-eruption conditions of Holocene dacite from Volcán San Pedro (36ºS, Chilean Andes) and the importance of sulphur in silicic subduction-related magmas. *Journal of Petrology* **45**, 855-881.

Courtillot, V. (1999). *Evolutionary catastrophes: the science of mass extinction.* Cambridge: Cambridge University Press, 171 p.

Courtillot, V. E. & Renne, P.R. (2003). On the ages of flood basalt events. *Comptes Rendus Geosciences* **335**, 113-140.

Crisp, J.A. & Spera, F.J. (1987). Pyroclastic flows and lavas of the Mogan and Fataga formations, Tejeda Volcano, Gran Canaria, Canary Islands: mineral chemistry, intensive parameters, and magma chamber evolution. *Contributions to Mineralogy and Petrology* **96**, 503-518.

Devine, J.D., Gardner, J.E., Brach, H.P., Layne, G.D. & Rutherford M.J. (1995). Comparison of microanalytical methods for estimation of H_2O contents of silicic volcanic glasses. *American Mineralogist* **73**, 845-9.

Dingwell, D.B., Holtz, F. & Behrens, H. (1997). The solubility of H_2O in peralkaline and peraluminous granitic melts. *American Mineralogist* **82**, 434-437.

Dingwell, D. B., Hess, K.U. & Romano, C. (1998). Extremely fluid behavior of hydrous peralkaline rhyolites. *Earth and Planetary Science Letters* **158**, 31-38.

Dixon, J.E., Stolper, E.M. & Holloway, J.R. (1995). An experimental study of water and carbon dioxide solubilities in mid-ocean ridge basaltic liquids. Part I: Calibration and solubility models. *Journal of Petrology* **36**, 1607-1631.

Dixon, J.E., Clague, D.A., Wallace, P. & Poreda, R. (1997). Volatiles in alkalic basalts from the North Arch volcanic field, Hawaii: extensive degassing of deep submarine-erupted alkalic series lavas. *Journal of Petrology* **38**, 911-939.

Eldholm, O. & Thomas, E. (1993). Environmental impact of volcanic margin formation. *Earth and Planetary Science Letters* **117**, 319-329.

Ewart, A., Milner, S.C., Armstrong, R.A. & Duncan, A.R. (1998). Etendeka volcanism of the Goboboseb mountains and Messum igneous complex, Namibia. Part I: voluminous quartz latite volcanism of the Awahab magma system. *Journal of Petrology* **39**, 227-253.

Ewart, A., Marsh, J.S., Milner, S.C., Duncan, A.R., Kamber, B.S. & Armstrong, R.A. (2004). Petrology and geochemistry of early Cretaceous bimodal continental flood volcanism of the NW Etendeka, Namibia. Part 2. Characteristics and petrogenesis of the high-Ti latite and high-Ti and low-Ti voluminous quartz latite eruptives. *Journal of Petrology* **45**, 107-138.

Gaillard F., Scaillet, B., Pichavant, M. & Bény, J.M. (2001). The effect of water and fO_2 on the ferric–ferrous ratio of silicic melts. *Chemical Geology* **174**, *255-273.*

Garland, F., Hawkesworth, C.J. & Mantovani, S.M. (1995). Description and petrogenesis of the Paraná rhyolites, Southern Brazil. *Journal of Petrology* **36**, 1193-1227.

Gerlach, T.M., McGee, K.A., Elias, T., Sutton, A.J. & Doukas, M.P. (2002). Carbon dioxide emission rate of Kilauea volcano: implications for primary magma and the summit reservoir. *Journal of Geophysical Research* **107**, 2189, doi:10.1029/2001JB000407.

Gwinn, R. & Hess, P. (1989). Iron and titanium solution properties in peraluminous and peralkaline rhyolitic liquids. *Contributions to Mineralogy and Petrology* **101**, 326-338.

Harris, C. & Erlank, A.J. (1992). The production of large-volume, low- $\delta^{18}O$ rhyolites during the rifting of Africa and Antarctica: the Lebombo Monocline, southern Africa. *Geochimica et Cosmochimica Acta* **56**, 3561-3570.

Harris, C. & Milner, S. (1997). Crustal origin of the Paraná rhyolites : discussion of « Description and petrogenesis of the Paraná rhyolites, Southern Brazil » by Garland *et al*. (1995). *Journal of Petrology* **38**, 299-302.

Holloway, J.R. (1987). Igneous fluids. In: Carmichael, I.S.E., & Eugster, H.P., (eds.), *Thermodynamic modelling of geological material*, *Reviews in Mineralogy* **17**, 211-232.

Jana, D. & Walker, D. (1997). The influence of sulfur on partitioning of siderophile elements. *Geochimica et Cosmochimica Acta* **61**, 5255-5277

Javoy, M. & Courtillot, V. (1989). Intense acidic volcanism at the Cretaceous-Tertiary boundary. *Earth and Planetary Science Letters* **94**, 409-416.

Jugo, P., Luth, R.W., & Richards, J.P. (2005). An experimental study of the sulfur content in basaltic melts saturated with immiscible sulfide or sulfate liquids at 1300°C and 1.0 Gpa. *Journal of Petrology*, **46**, 783-798.

Keppler, H. (1999). Experimental evidence for the source of excess sulfur in explosive volcanic eruption. *Science* **284**, 1652-1654.

Kilpatrick, J.A. & Ellis, D.A. (1992). C-type magmas: igneous charnockites and their extrusive equivalents. *Transactions of the Royal Society of Edinburgh* **83**, 155-164.

King, P.L., White, A.J.R., Chappell, B.W. and Allen, C.M. (1997) Characterization and origin of aluminous A-type granites from the Lachlan Fold Belt, southeastern Australia. *Journal of Petrology*, **38**, 371-91.

Kirstein, L.A., Hawkesworth, C.J. & Garland, F. (2001). Felsic lavas or rheomorphic ignimbrites: is there a chemical distinction? *Contributions to Mineralogy and Petrology* **142**, 309-322.

Kracher, A. & Wasson, J. (1982). The role of S in the evolution of the parental cores of the iron meteorites. *Geochimica et Cosmochimica Acta* **46**, 2419-2426.

Kress, V.C. & Carmichael, I.S.E. (1991). The compressibility of silicate liquids containing Fe_2O_3 and the effect of composition, temperature, oxygen fugacity and pressure on their redox states. *Contributions to Mineralogy and Petrology* **108**, 82-92.

Lange, R.A. (2002). Constraints on the pre-eruptive volatile concentrations in the Columbia River flood basalts. *Geology* **30**, 179-182.

Lightfoot, P.C., Hawkesworth, C.J. & Sethna, S.F. (1987). Petrogenesis of rhyolites and trachytes from the Deccan trap : Sr, Nd and Pb isotope and trace element evidence. *Contributions to Mineralogy and Petrology* **95**, 44-54.

Linnen, R. & Keppler, H. (2002). Melt composition control of Zr/Hf fractionation in magmatic processes. *Geochimica et Cosmochimica Acta* **66**, 3293-3301.

Lowenstern, J.B., Mahood, G.A., Hervig, R.L. & Sparks, J. (1993). The occurrence and distribution of Mo and molybdenite in unaltered peralkaline rhyolites from Pantelleria, Italy. *Contributions to Mineralogy and Petrology* **114**, 119-129.

Luhr, J.F. (1990). Experimental phase relations of water- and sulfur-saturated arc magmas and the 1982 eruptions of El Chichon volcano. *Journal of Petrology* **31**, 1071-1114.

Macdonald, R., Smith, R.L. & Thomas, J.E. (1992). Chemistry of the subalkalic silicic obsidians. *U.S. Geological Survey Professional Paper* **1523**, 214pp.

Mahood, G.A. (1984). Pyroclastic rocks and calderas associated with strongly peralkaline magmatism. *Journal of Geophysical Research* **89**, 8540-8552.

Métrich, N., Sigurdsson, H., Meyer, P.S. & Devine, J.D. (1991). The 1783 Lakagigar eruption in Iceland: geochemistry, CO_2, and sulfur degassing. *Contributions to Mineralogy and Petrology* **107,** 435-447.

Moore, G., Righter, K. & Carmichael, I.S.E (1995). The effect of dissolved water on the oxidation state of iron in natural silicate liquids. *Contributions to Mineralogy and Petrology* **120**, 170-179.

Morgan, W.J. (1981). Hot spot tracks and the opening of the Atlantic and Indian oceans, In: Emiliani, C. (ed.) *The Sea, Vol. 7*. New York: Wiley Interscience, 443-487.

Morgan, J.P., Reston, T.J. & Ranero, C.R. (2004). Contemporaneous mass extinctions, continental flood basalts, and impact signals : are mantle plume-induced lithospheric explosions the causal link ? *Earth and Planetary Science Letters* **217**, 263-284.

Mungall J.E. & Martin, R.F. (1996). Extreme differentiation of peralkaline rhyolite, Terceira, Azores: a modern analogue of Strange Lake, Labrador? *The Canadian Mineralogist* **34**, 769-777.

Mysen, B.O. (1988). *Structure and properties of silicate melts*. New York: Elsevier, 388 pp.

Nekvasil, H., Dondolini, A., Horn, J., Filiberto, J., Long, H. & Lindsley, D.H. (2004). The origin and evolution of silica-saturated alkalic suites: an experimental study. *Journal of Petrology* **45**, 693-721.

O'Neill, H.St. & Mavrogenes, J.A. (2002). The sulfide capacity and the sulfur content at sulfide saturation of silicate melts at 1400°C and 1 bar. *Journal of Petrology* **43**, 1049-1087.

Peccerillo, A., Barberio, M.R., Yirgu, G., Ayalew, D., Barbieri, M. & Wu, T.W. (2003). Relationships between mafic and peralkaline silicic magmatism in continental rift settings: a petrological, geochemical and isotopic study of the Gedemsa volcano, Central Ethiopia Rift. *Journal of Petrology* **44**, 2003-2032.

Poulson, S.R. & Ohmoto, H. (1989). Devolatilization equilibria in graphite-pyrite-pyrrhotite bearing pelites with application to magma-pelite interaction. *Contributions to Mineralogy and Petrology* **101**, 418-425.

Rampino, M.R. & Self, S. (1992). Volcanic winter and accelerated glaciation following the Toba super-eruption. *Nature* **359**, 50-52.

Rampino, M.R. & Self, S. (2000). Volcanism and biotic extinctions. In: Sigurdsson, H. (ed) *Encyclopedia of Volcanoes*. San Diego: Academic Press, 1083-1094.

Robie, R.A., Hemingway, B.S., & Fisher, J.R. (1979). Thermodynamic properties of minerals and related substances at 298.15 K and 1 bar (10^5 Pascals) pressure and at higher temperature. *US Geological Survey Bulletin*. **1452**.

Robock, A. (2000). Volcanic eruptions and climate. *Reviews of Geophysics* **38**, 191-219.

Rochette, P., Tamrat, E., Féraud, G., Pik, R., Courtillot, V., Ketefo, E., Coulon, C., Hoffmann, C., Vandamme, D. & Yirgu, G. (1998). Magnetostratigraphy and timing of the Oligocene Ethiopian traps. *Earth and Planetary Science Letters* **164**, 497-510.

Rodriguez Durand, S. & Sen, G. (2004). Preeruption history of the Grande Ronde Formation lavas, Columbia River Basalt Group, American Northwest : evidence from phenocrysts. *Geology* **32**, 293-296.

Scaillet, B., Clemente, B., Evans, B.W. & Pichavant, M. (1998). Redox control of sulfur degassing in silicic magmas. *Journal of Geophysical Research* **103**, 23937-23949.

Scaillet, B. & Evans, B.W. (1999). The 15 June 1991 eruption of Mount Pinatubo. I. Phase equilibria and pre-eruption P-T-fO_2-fH_2O conditions of the daite magma. *Journal of Petrology* **40**, 381-411.

Scaillet, B. & Macdonald, R. (2001). Phase relations of peralkaline silicic magmas and petrogenetic implications. *Journal of Petrology* **42**, 825-845.

Scaillet, B. & Macdonald, R. (2003). Experimental constraints on the relationships between peralkaline rhyolites of the Kenya rift valley. *Journal of Petrology* **44**, 1867-1894.

Scaillet, B. & Pichavant, M. (2003). Experimental constraints on volatile abundances in arc magmas and their implications for degassing processes. In: Oppenheimer, C., Pyle, D.M. & Barclay, J. (eds) *Volcanic Degassing*. *Geological Society Special Publication* **213**, 23-52.

Scaillet, B. & Pichavant, M. (2004). Role of fO_2 in fluid saturation of oceanic basalt. *Nature*, doi.org/10.1038/nature02814

Scaillet, B. & Pichavant, M. (2005). A model of sulphur solubility for hydrous mafic melts : application to the determination of magmatic fluid compositions of Italian volcanoes, *Annals of Geophysics,* **48**, 671-698.

Scaillet, B., Luhr, J.F. & Carroll, M.C. (2003). Petrological and volcanological constraints on volcanic sulfur emissions to the atmosphere. In: Robock, A. & Oppenheimer, C. (eds) *Volcanism and the Earth's Atmosphere*. *Geophysical Monograph* **139**, 11-40.

Scaillet, B., Pichavant, M., Roux, J., Humbert, G. & Lefèvre, A. (1992). Improvements of the Shaw membrane technique for measurement and control of fH_2 at high temperatures and pressures. *American Mineralogist* 77, 647-655.

Scarfe, C.M. (1977). Viscosity of a pantellerite melt at one atmosphere. *Canadian Mineralogist* **15**, 185-189.

Schmidt, B.C., Scaillet, B. & Holtz, F. (1995). Accurate control of fH_2 in cold seal pressure vessels with the Shaw membrane technique. *European Journal of Mineralogy* 7, 893-903.

Sharma, K., Blake, S., Self, S. & Krueger, A.J. (2004), SO_2 emissions from basaltic eruptions, and the excess sulfur issue, *Geophysical Research Letters*, *31*, L13612, doi:10.1029/2004GL019688.

Shi, P. (1992). Fluid fugacities and phase equilibria in the Fe-Si-O-H-S system. *American Mineralogist* **77**, 1050-1066.

Sparks, R.J.S., Bursik, M.I., Carey, S.N., Gilbert, J.S., Glaze, L.S., Sigurdsson, H. & Woods, A.W. (1997). *Volcanic Plumes*. Wiley, 574 pp.

Stone, R. (2004). Iceland's doomsday scenario? *Science* **306**, 1278-1281.

Thordarson, T. & Self, S. (2003). Atmospheric and environmental effects of the 1783-1784 Laki eruption : a review and reassessment. *Journal of Geophysical Research* **108** (D1) 4011, doi : 10.1029/2001JD002042.

Thordarson, T., Self, S., Oskarsson, N. & Hulsebosch, T. (1996). Sulfur, chlorine, and fluorine degassing and atmospheric loading by the 1783-1784 AD Laki (Skaftar Fires) eruption in Iceland. *Bulletin of Volcanology* **58**, 205-225.

Touchard, Y., Rochette, P., Aubry, M.P. & Michard, A. (2003). High resolution magnetostratigraphic and biostratigraphic study of Ethiopian traps-related products in Oligocene sediments from the Indian ocean. *Earth and Planetary Science Letters* **206**, 493-508.

Trua, T., Deniel, C. & Mazzuoli, C. (1999). Crustal control in the genesis of Plio-Quaternary bimodal magmatism of the main Ethiopian Rift (MER): geochemical and isotopic (Sr, Nd, Pb) evidence. *Chemical Geology* **155**, 201-231.

Vogt, P.R. (1972). Evidence for global synchronism in mantle plume convection, and possible significance for geology. *Nature* **240**, 338-342.

Wallace, P. (2002). Volatiles in submarine basaltic glasses from the Northern Kerguelen plateau (ODP site 1140): implications for source region compositions, magmatic processes, and plateau subsidence. *Journal of Petrology* **43**, 1311-1326.

Watson, E.B. (1979). Zircon saturation in felsic liquids: experimental results and application to trace element geochemistry. *Contribution to Petrology and Mineralogy* **70**, 407-419.

Watson, E.B. (1994). Diffusion in volatile-bearing magmas. In: Carroll, M.R. & Holloway, J.R. (eds) *Volatiles in Magmas. Reviews in Mineralogy* **30**, 371-411.

Webster, J.D., Taylor, R.P. & Bean, C. (1993) Pre-eruptive melt composition and constraints on degassing of a water-rich pantelleritic magma, Fantale volcano, Ethiopia. *Contributions to Mineralogy and Petrology* **114**, 53-62.

Wedepohl, K.H. (1995). The composition of the continental crust. *Geochimica et Cosmochimica Acta* **59**, 1217-1232.

White, J.C., Ren, M. & Parker, D.F. (2005). Variation in mineralogy, temperature, and oxygen fugacity in a suite of strongly peralkaline lavas and tuffs, Pantelleria, Italy. *The Canadian Mineralogist* **43**, 1331-1347

Wignall, P.B. (2001). Large igneous provinces and mass extinctions. *Earth Science Reviews* **53**, 1-33.

Woods, A.W. (1993). A model of the plumes above basaltic fissure eruptions. *Geophysical Research Letters* 20, 1115-1118.

Xu, Y., Chung, S.L., Jahn, B.M. & Wu, G. (2001). Petrological and geochemical constraints on the petrogenesis of Permian-Triassic Emeishan flood basalts in southwestern China. *Lithos* **58**, 145-168.

Zhang, Y. (1999). H_2O in rhyolitic glasses and melts: measurement, speciation, solubility, and diffusion. *Reviews in Geophysics* **37** (4), doi:10.1029/1999RG900012.

Captions to figures.

Figure 1. Sulphur behaviour in peralkaline rhyolites with 1 wt% sulphur at 800°C and 150 MPa. (**a**) Melt sulphur content as a function of fO_2 for the three rhyolite compositions of increasing peralkalinity (ND < SMN < EBU) used in the experiments (Table 2). Also shown are the sulphur contents of metaluminous silicic melts (MET) held under similar P-T-S_{bulk} conditions (Luhr, 1990; Scaillet *et al*., 1998). The maximum error on fO_2 is 0.3 log unit. **(b)** Variations in the S_{fluid}/S_{melt} partition coefficient with fO_2 for the three peralkaline rhyolites with *c.* 1 wt% bulk sulphur. Two error bars are shown, one for partition coefficients lower than 100 (bottom part) and one for partition coefficients at around 300 (middle part). Each error bar represents an uncertainty of *c*. 50%. For clarity, the error bar corresponding to the EBU datum at 550 (±275) is not reported. (**c**) Variation of the proportion of sulphide (wt% Po = mass Po / (mass of Po + mass of hydrous melt)) with fO_2 in the three peralkaline rhyolites. Also shown is the proportion of sulphide in the Pinatubo dacite (MET) with *c*. 1 wt% bulk sulphur held over the same fO_2 range at 780°C (Scaillet *et al*., 1998). The cross represents the typical error on calculated wt% Po and experimental fO_2.

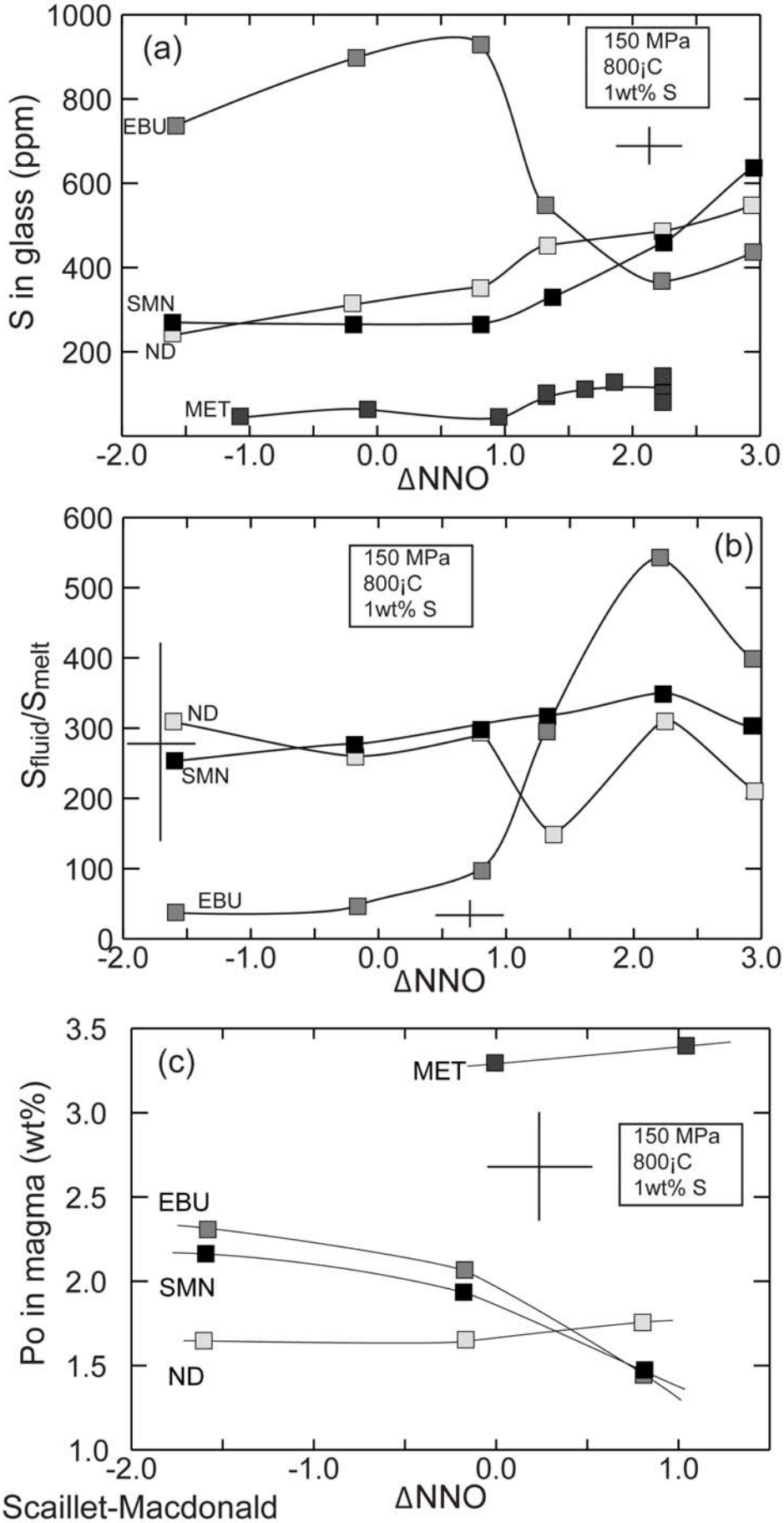

Fig. 1, Scaillet-Macdonald

Figure 2. Variation in the melt sulphur content of EBU rhyolite with the bulk S content for two different temperatures, both at an fO_2 of *c*. NNO-1.6.

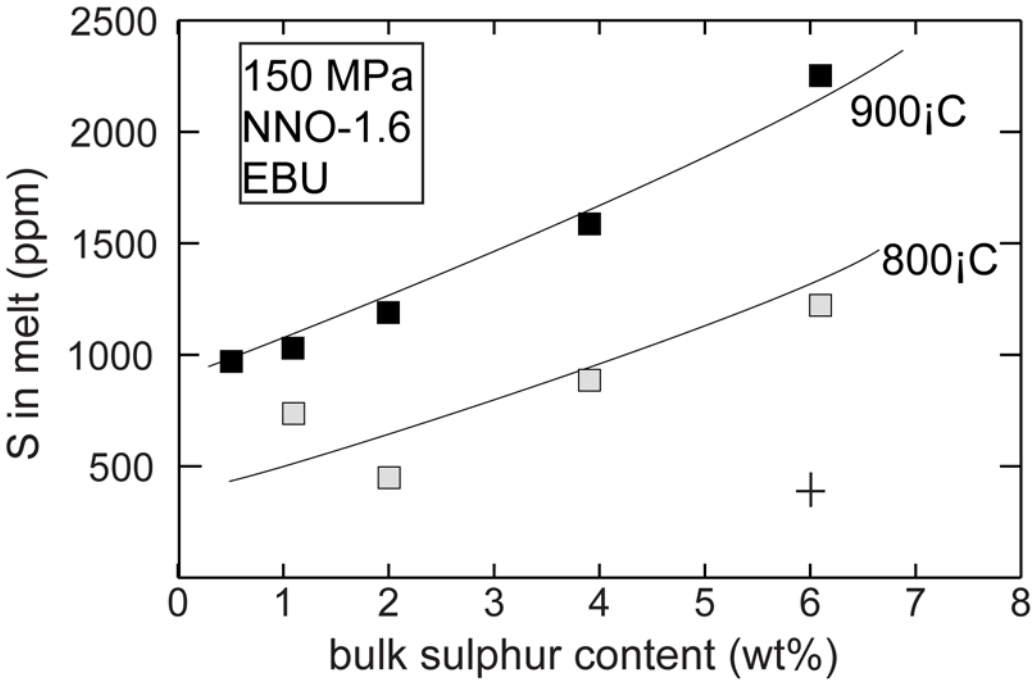

Fig. 2, Scaillet-Macdonald

Figure 3. Variation in the S_{fluid}/S_{melt} partition coefficient with increasing bulk S content for the EBU rhyolite at 800 and 900°C at three fO_2. Two error bars are shown, one for partition coefficients lower than 100 (bottom part) and one for partition coefficients at around 300 (middle part). Each error bar represents an uncertainty of *c*. 50%. For clarity, the error bar corresponding to data at c. 400 is not reported.

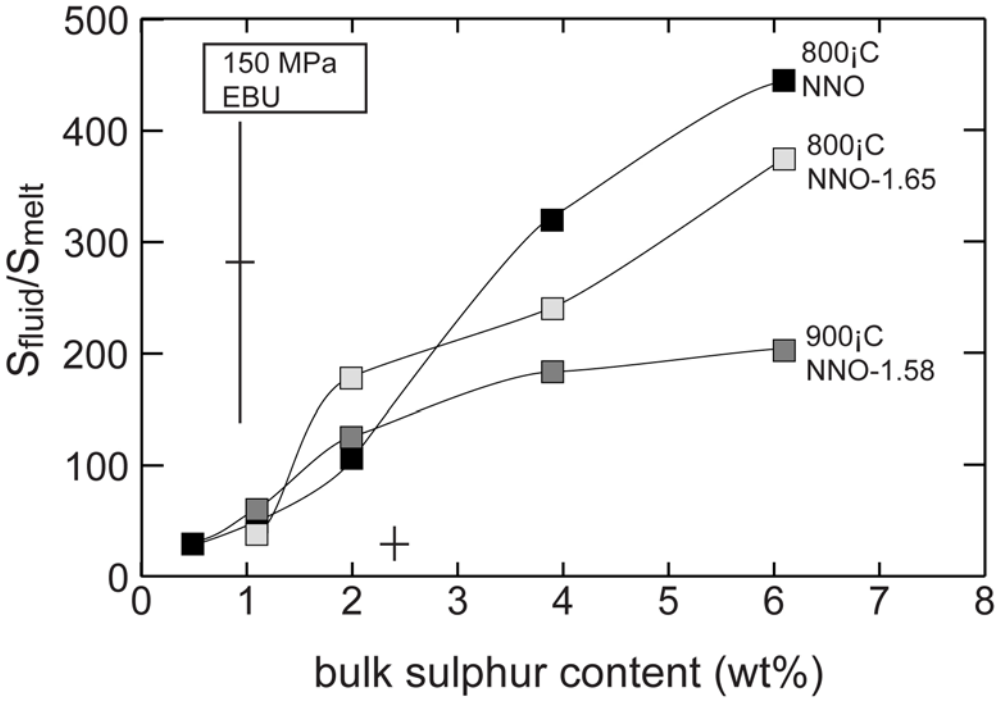

Fig. 3, Scaillet-Macdonald

Figure 4. Variations in sulphide activity (in log scale, log(*a*FeS)) in the melt during the crystallisation of a basalt magma for different fO_2. (**a**) with 1 wt% H_2O and 1000 ppm sulphur. The decrease of *a*FeS observed at high melt fractions is due to the fact that intermediate compositions are Fe-rich compared to the parent magma, and thus have a higher sulphur solubility (which consequently induces a decrease in *a*FeS) than the totally molten starting magma. (**b**) with 1 wt% H_2O, 1 wt% CO_2 and 1000 ppm sulphur. Note that at NNO-2, the magma does not reach sulphide saturation even after 80% crystallisation. In all calculations we assume that, once stable, the sulphide melt is made of pure FeS and we thus neglect the role of Ni.

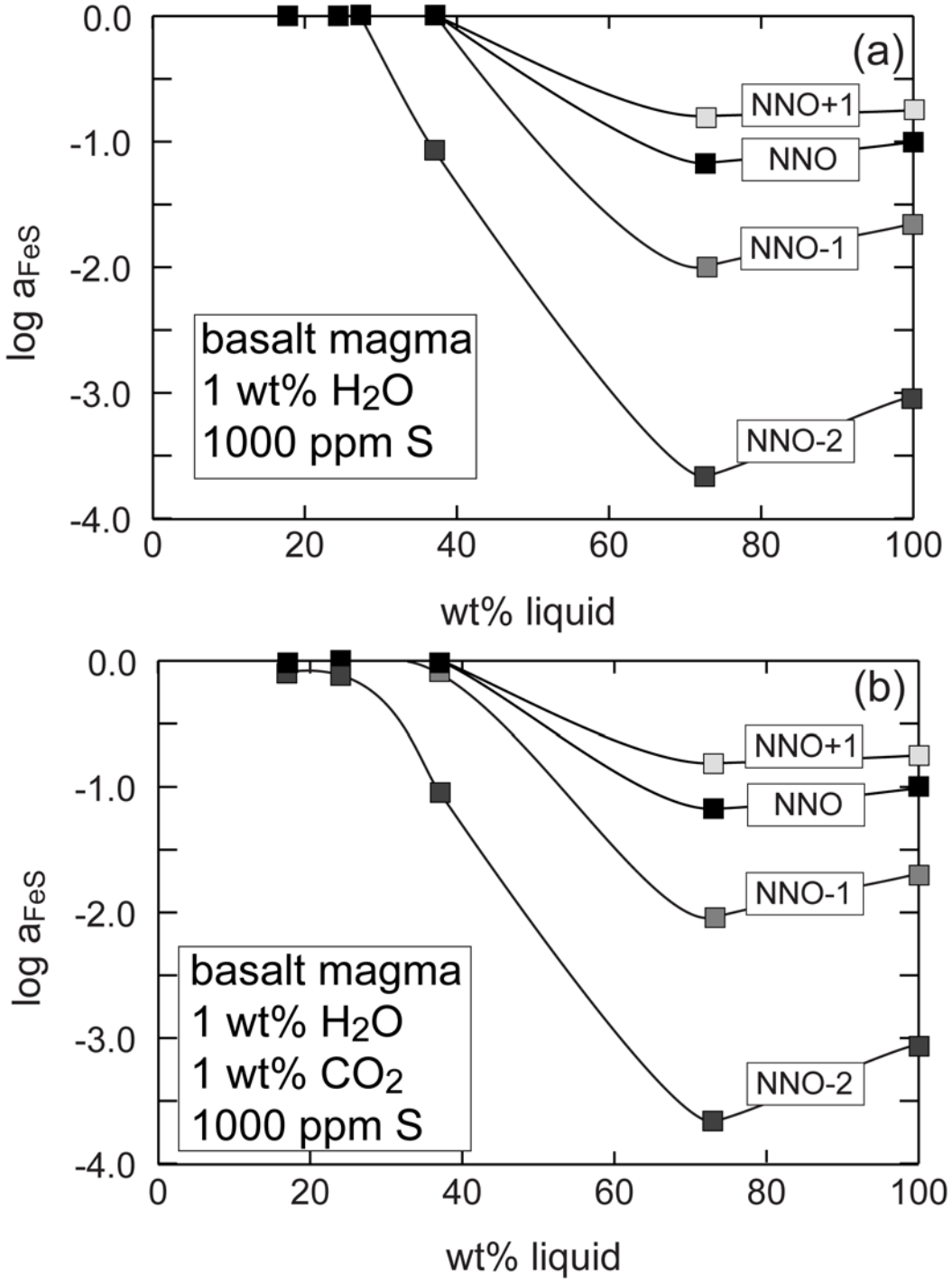

Fig. 4, Scaillet-Macdonald

Figure 5. Relative amounts of sulphur hosted in the sulphide and in the fluid in a crystallising basalt with 1000 ppm sulphur. (**a**) Proportion of bulk sulphur locked in sulphide during the crystallisation of a hydrous basalt (1 wt% H_2O), calculated for 4 different fO_2. Under these conditions (i.e. no CO_2 present) there is no

fluid phase so the the remaining sulpur is in the residual melt. (**b**) Proportion of bulk sulphur dissolved in the fluid during the crystallisation of a H_2O-CO_2 bearing basalt calculated for various fO_2. The presence of CO_2 promotes early fluid saturation and, as a result, a significant part of the sulphur present in the system goes into the fluid phase. The curve labelled 2 wt% H_2O+CO_2 corresponds to the case where the bulk H_2O and CO_2 are each set at 2 wt%. All other curves are for 1 wt% H_2O and 1 wt% CO_2.

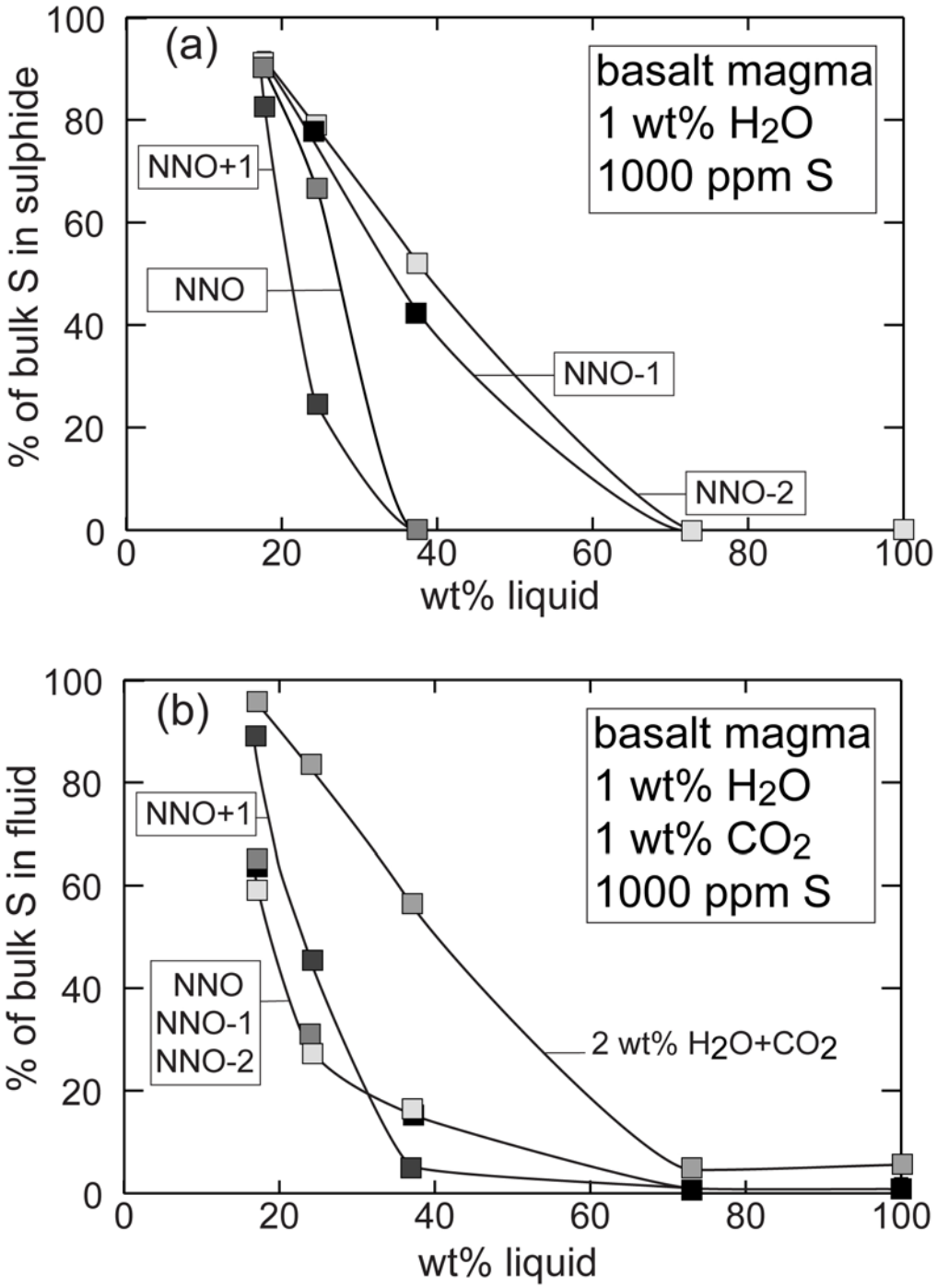

Fig. 5, Scaillet-Macdonald

Figure 6. Effect of bulk H_2O and CO_2 contents on the sulphide activity (log scale) of a crystallising basalt at an fO_2 of NNO-2. Note that when there is a large amount of CO_2 in the magma (i.e. the 2 wt% case), the coexisting fluid can scavenge a significant proportion of the bulk sulphur such that the system does not reach saturation in sulphide even after 80% of crystallisation.

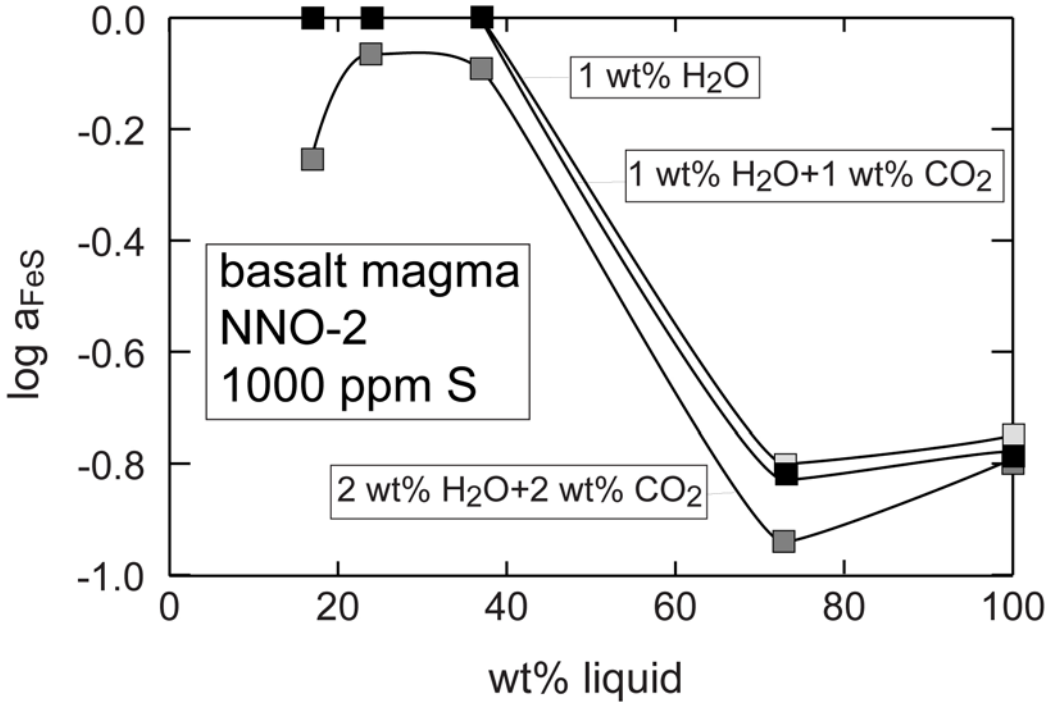

Fig. 6, Scaillet-Macdonald

Figure 7. Sulphur content of crustal melts produced during partial melting of previously dehydrated hot lower crust, such as proposed for the origin of the Etendeka-Parana flood rhyolites. (**a**) Variation with fO_2 of the melt sulphur content of H_2O-poor metaluminous rhyolitic magmas, calculated for three different bulk melt water contents, using the solubility model of Clemente *et al.* (2004). In all cases the sulphur fugacity has been set at 0.1 MPa. (**b**) Sulphur content of a C-O-H-S metamorphic fluid, calculated for various mole fraction of H_2O (i.e. various fH_2O) in the fluid, three different fO_2 and an fS_2 of 0.1 MPa, which corresponds to the pyrite-pyrrhotite equilibrium (Shi, 1992). The calculations are done using an MRK equation of state (Holloway, 1987). The difference to 100 % on the ordinate scale corresponds to fluid species other than S and H_2O, i.e., CO_2, CO, CH_4.The sulphur contents of the fluid are intended to model the sulphur content of

putative metamorphic fluids that have scavengend the lower crust from most of its volatiles prior to widespread melting.

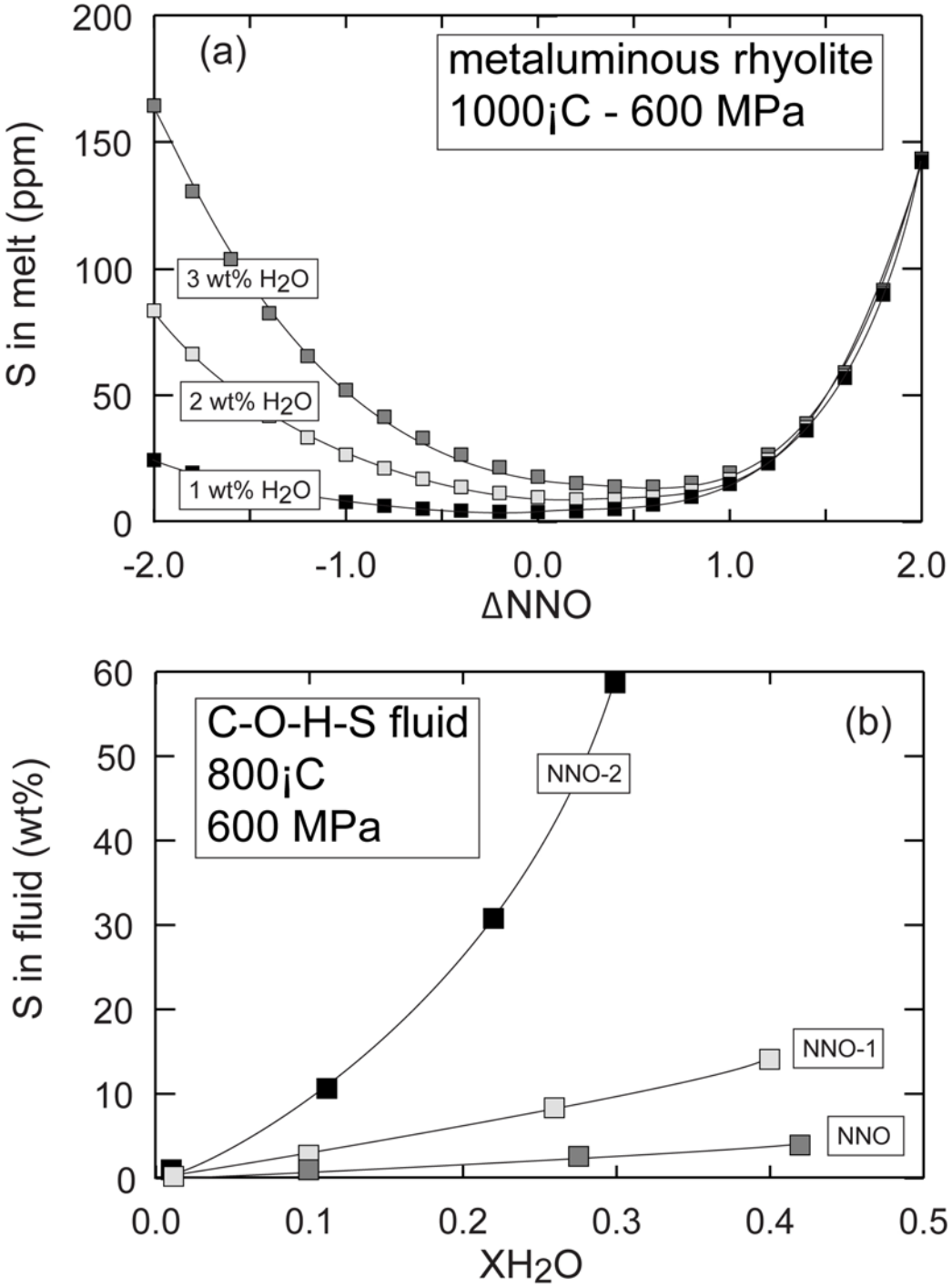

Fig. 7, Scaillet-Macdonald